University of Southern Queensland

Faculty of Engineering & Surveying

Fracture Analysis of Vinyl Ester Composites Under Microwave Condition

A dissertation submitted by

Shing Hin Tsang

in fulfillment of the requirements of

ENG4112 Research Project

towards the degree of

Bachelor of Engineering (Electrical and Electronic)

Submitted: October, 2004

Abstract

Vinyl ester (VE) with 33% Flyash composite has been widely used in the construction industry due to its superiority material properties but these composites suffer considerable shrinkage during the curing and hardening processes. Some researchers have proven that vinyl ester composite cured under microwave heat treatment will reduce the shrinkage problem. This purpose of this project is to research, measure and compare the fracture toughness of vinyl ester composite cured under ambient and microwave conditions by using the short bar test. Furthermore, the fracture surface is investigated by using the Scanning Electron Microscope (SEM).

The specimens were fractured by using the MTS 810 Material Testing Systems and the value of fracture toughness was obtained through some calculations. The result was further proven from the SEM microscopy analysis where the lower value of fracture toughness specimen will have more microvoid or bubbles comparing to the specimen with the higher value of fracture toughness.

The result analysis tool called Latin Squares was used to determine which treatments were most effective in maintaining the fracture toughness while reducing the shrinkage of vinyl ester composite, and by how much, and which are worthless, so we can weight the economic alternatives.

Keywords: Vinyl Ester, Shrinkage, Fracture Toughness, Short Bar Test, Scanning Electron Microscope, MTS 810, Microvoid, Latin Squares,

Declaration

University of Southern Queensland

Faculty of Engineering and Surveying

ENG 4111 and ENG 4112 Research Project

Limitations of Use

The Council of the University of Southern Queensland, its Faculty of Engineering and Surveying, and the staff of the University of Southern Queensland, do not accept any responsibility for the material associated with or contained in this dissertation.

Persons using all or any part of this dissertation do so at their own risk, and not at the risk of the Council of the University of Southern Queensland, its Faculty of Engineering and Surveying or the staff of the University of Southern Queensland. The sole purpose of the unit entitled "Project" is to contribute to the overall education process designed to assist the graduate enter the workforce at a level appropriate to the award.

The project dissertation is the report at of an educational exercise and the document, associated hardware, drawings, and other appendices or parts of the project should not be used for any other purpose. If they are so used, it is entirely at the risk of the user.

Graham Baker.

Prof G Baker
Dean
Faculty of Engineering and Surveying

Certification

I certify that the ideas, designs and experimental work, results, analyses and conclusions set out un this dissertation are entirely my own effort, except where otherwise indicated and acknowledged.

I further certify that the work is original and has been previously submitted for assessment in any other course or institution, except where specifically stated.

Shing Hin Tsang

Student Number: D1232992

_____ Signature

_____ Date

Acknowledgment

I would like to take this opportunity to say my deep appreciation and thank you to the peoples that has assisted me in doing this Engineering Research Project.

Firstly a big thanks you to my project supervisors – Dr. Harry Ku, Mr. Doug Baddeley and Mr. Chris Snook for guiding me in doing this whole project from the starts. Thank you for your advice, teaching, guidance and expertise.

I would also like to say thank you all technicians for assisting in setting up the equipment and providing information especially to Mr. Mohan Trada, from the Faculty Research Technician for his patience and assistance.

Secondly a big thank you to Queensland University of Technology (QUT), in lending me their Scanning Electron Microscope (SEM) as a reference for this research project.

Lastly to other individuals namely Kenny Lim and Lenore Lee, in their assistance and support in doing this research project.

Table of Contents

Appendix

540-Watts 20 Seconds:

540-Watts 25 Seconds:

720-Watts 15 Second:

720-Watts 20 Second:

720-Watts 25 Second:

540-Watts 25 Second:

List of Figures:

List of Tables

Chapter 1. Introduction

1.1 History and commercial of Vinyl Ester

Composite offers desirable mechanical properties, long-term durability, and fabrication flexibility. The most common composite matrices are unsaturated polyesters, epoxies and vinyl esters. Usually, epoxies are used in high-performance applications. The unsaturated polyesters are commonly used. It dominates the market because of its low price, reasonably good material properties and the simple processing. However, the basic unsaturated polyester formulations have limitation of poor temperature and ultra-violet tolerance. The use of additives is to reduce these disadvantages in order to suit the most applications. Mechanical properties and temperature tolerance of unsaturated polyesters are no longer be adequate as epoxies are often used, due to their significant superiority in these respects. Certainly, these improved properties are very costly and epoxies are only applicable in the environment where the cost tolerance is high.

Vinyl ester resins are addition to the products of various epoxies resins and unsaturated monocarboxylic acids where these are the most common materials to be mixed with acrylic acid. Vinyl ester was developed in the 1960s. Vinyl ester resins can be easy handling in room's temperature combined with the best properties of epoxies and unsaturated polyesters. The temperature and mechanical properties are similar to epoxies resins. They have better chemical resistance than cheaper polyester resins. Vinyl Ester (VE) is chemically related to both unsaturated polyesters and epoxies, in most respects

represent comprise between the two. They were developed in an attempt to combine the fast and simple cross linking of unsaturated polyesters with the mechanical and thermal properties of epoxies.

The composites made from vinyl ester resins by the Fibre Composite Design and Development (FCDD) group as the University of Southern Queensland (USQ) endure the considerable shrinkage during hardening. This particular shrinkage is considered as serious matter when the composite components are in large size. It can be more than ten percent, which is much higher than claimed by some researchers and resins' manufacturers (Clarke, 1996; Matthews, 1994). The main problems of this shrinkage in the composite component are the stresses set up internally. These stresses are usually tensile in the core of the component and compressive on the surface (Osswald, 1995). These may occur when the stresses operate together with the applied loads during service. Thus, it causes a premature failure of the composite components. The Fibre Composite Design and Development (FCDD) group has solved this shrinkage problem by breaking a large composite into smaller composite parts. This is because of the smaller composite parts that have less shrinkage where these smaller parts are then joined together to create the overall structure. The diagram of this shown in Figure 1.1, these all are the individual items of the components that are manufactured by casting liquid form, uncured 44% by volume or 33% by weight flyash particulate reinforced vinyl esters [VE/FLYASH (33%)] into moulds. By doing so, the manufacturing lead-time and costs of a composite component will be considerably increased.

1.2 Overview of Fracture Mechanics

Pressure vessels, ship hulls and aircraft structures, which are categorised as fractures of well-designed structures, can sometimes occur at stresses well below the yield strength of the structural materials. With this, there is an unknown property missing because these structures had been designed well within material property limits. Conventional design procedures were analysed and it was found that the facts that flaws might exist in the material were not considered. This is where the research into the field of fracture mechanics was started.

The determination of severity of a pre-existing defect in terms of its tendency to initiate a fracture that would cause failure is the aim of fracture mechanics. K_{IC}, which is the critical fracture toughness value, can be used to improve the reliability of a component or structure. In determining K_{IC} value of a material, the standard testing procedure is being use and is necessary. Two standards are available which The American Society for Testing and Material (ASTM) procedure E399-83 is the first and secondly is the British Standard test procedure BS: 5447. These standards assign restrictions on the dimension of a sample and how it should be prepared. Therefore by having these restrictions, the testing procedure tends to be very expensive.

However, to overcome this, Barker has developed a short rod or bar test to address the problems associated with the standard test methods (Baker 1977). Here smaller and cheaper samples can be tested, using the short rod/bar test method. With this, it the test will be more applicable to be used as quality control test on manufactured item such as on

medium to large size construction components. Since it is known that the properties of component largely dependant on the fracture toughness, a better quality control would be available if the fracture toughness of a component could be determined easily. Therefore for this situation the short rod/bar is the best used to test the quality of the component.

1.3 Project aim and Specific Objectives

During the curing process the vinyl ester suffers will occur shrinkage. Therefore microwave energy in multimode oven cavity is to be applied to samples the vinyl ester resins under controlled conditions to minimize its shrinkage. By this a commercial 1.8 kW microwave oven is used. By launching the microwave from two 0.9-kW magnetrons, a 1.8kW power will be achieved. Power inputs can vary from 10% (180 W) to 100% (180 W) in term of each step with 180 W. Thus, the material properties may change when vinyl ester composites are cured under microwave condition; these can be the due to the increase of flaw in the material and so on.

As of this, the aim of this project is to use short bar test to forecast the critical fracture toughness, K_{IC} for the material of vinyl ester cured under ambient and varied type of microwave conditions. While the fracture surfaces of specimen is being analysed by using Electron Scanning Microscope (SEM) to investigate the fracture properties of vinyl ester composites deeply, Latin square, would be used for the statistical experiment in order to interpret and analyse the result in a more simple and comprehensive way. Latin square is a multiplication table in the form of a matrix. From here, the outcome obtained

is being expected to assist the FCDD group or other construction company in using vinyl ester composites. Hence, vinyl ester composites can be widely used, as it could replace other materials because of its superior material properties and also it is cheap.

1.4 Dissertation Overview

In summary chapter 1 gave a brief application of vinyl ester outline and fracture mechanics while the result analysis tool which is called Latin squares is being introduced. Here it gives a rough idea of how the result will be analysed. Here too the aim and objectives of this project is being stated. In chapter 2, the vinyl ester composites and the usage of microwave in detail has being described. In addition the issue on health in context upon using the chemical materials is also being discussed in the same chapter. Then in the next chapter, the fractures mechanics has been discussed on the issues that are importance, the theories to be used and also application. For chapter 4, the fracture toughness test methods have been discussed in dept, which included the standard and non-standard test methods. Also the analysis methods for brittle and ductile material are being described in this chapter. In Chapter 5 it described the short rod or bar test method in detail, as it would be chosen for the analysis fracture in this project. The main source of this chapter is the journal published by Barker in 1981. Then chapter 6 discussed the ways of preparing the microwave heat treatment and the short specimen. Photos were taken during the experiment as it shows in the illustrating of the procedures clearly. The test rigs and equipments used in the project was the main topic for chapter 7. Several test rigs have been mentioned but only the MTS 810 Material Testing System was chosen.

The reason for choosing it or other equipments and their operations are the issues to be concerned in this chapter too. Then some introduction to the result analysis tool called Latin square and the example for the calculation of result was demonstrated step by step were then mention in Chapter 8. In Chapter 9, the experimental result and discussion is has been stated which involved the result obtained from the tensile testing, SEM analysis and the analysis of Latin squares. Lastly, the conclusion and recommendation for result improvement is on chapter 10. All graphs and table have statistically illustrated the result and discussion. However the recommendation and conclusion were drawn from the experiences in doing this project and also expert advices from the concerned area. Project specification, drawings, result data and SEM images results is being attached in the appendix section.

Chapter 2. Composite Material and Interactions with Microwave

2.1 Introduction of Vinyl Ester Resins and Their Cross Linking

Vinyl ester resins are addition products of various epoxies resins and unsaturated monocarboxylic acids, most commonly met acrylic acid. It was developed in 1960s. Vinyl ester resins can be easily handled at room combine the best properties of epoxies and unsaturated polyesters. They temperature and have mechanical properties similar to epoxy resins. They have better chemical resistance than cheaper polyester resins, especially hydrolytic stability, and at the same time offer greater control over cure rate and reaction conditions than epoxy resins. The unsaturated bonds on the termini of the vinyl ester with the co monomer to form a cross linked network similar to the curing reactions of unsaturated polyesters. Vinyl ester resins are similar to unsaturated polyester resins in that both systems contain styrene monomer as reactive diluents and that both unsaturated polyester and vinyl esters provide crosslink sites. Vinyl esters have reactive double bonds at the ends of the chains only, while the unsaturated polyester resins have the reactive double bonds distributed throughout the chains. Thus, the crosslink density can be better controlled in the vinyl esters. This chapter is designed to review recent developments in the field of vinyl ester resins including crosslinking mechanism, overview of microwave, interactions with microwave, risk of styrene and MEKP.

2.2 Cross Linking of Vinyl Ester Resins

2.2.1. Initiators Crosslinking Reactions

The crosslinking reactions of vinyl ester resins are initiated by free radicals. Free radicals are generated in several ways, including thermal or photochemical decomposition of peroxides and hydroperoxides or azo and diazo compounds. The type of vinyl ester resins, the method of fabrication and the requirements of the application determine the uses of initiator systems. The initiators most commonly used for vinyl ester resin cure reactions are methyl ethyl ketone peroxide (MEKP), benzoyl peroxide and cumene hydroperoxide. Decomposition of these initiators can be effected by heat or by the use of accelerators or promoters, which can cause a more rapid decomposition of the initiator at a given temperature. The accelerators most commonly employed are tertiary amines, such as dimethyl- or diethyl- aniline, and metallic soaps, such as cobalt or manganese octoate or naphthenate. Vinyl ester resins can also be crosslinked via ionizing radiation - either actinic or high energy. Electron radiation has such high quantum energy that the free radicals required for polymerization are formed directly from the vinyl ester resin.

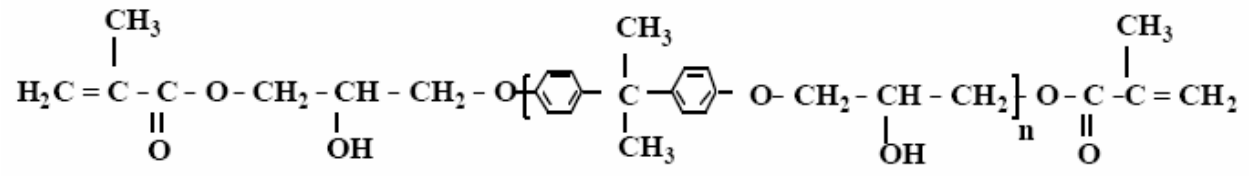

Figure 2.1. The structure of the vinyl ester reactants

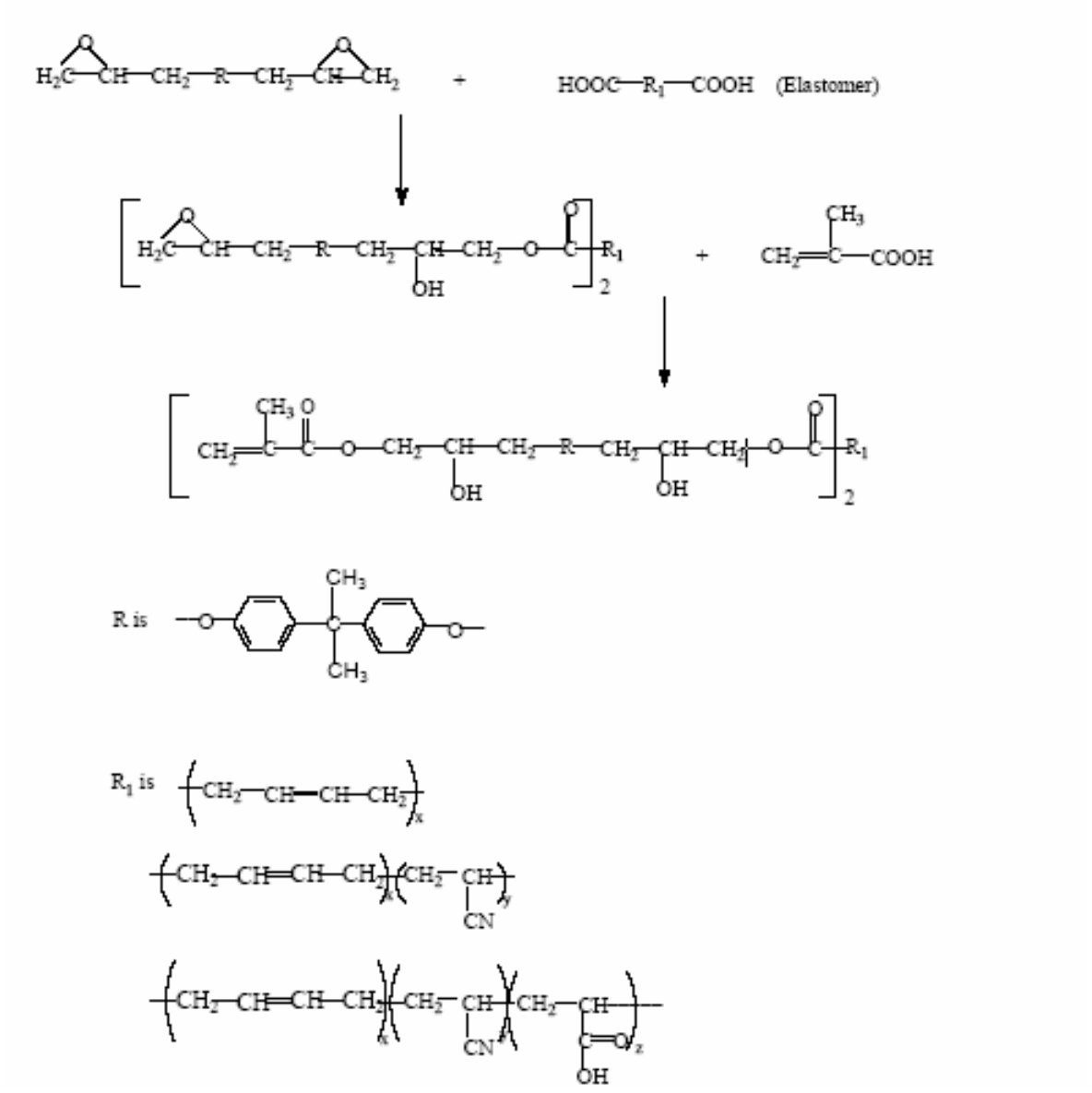

Figure 2. 2. Preparation of toughened vinyl ester resins.

2.2.2. Crosslinking Reaction

Vinyl ester resins are crosslinked by free radical copolymerization of methacrylate end groups with styrene. It is a system of copolymerization of vinyl/divinyl monomers. Figure 2.1 shows a schematic representation of the network formed by the free radical crosslinking reaction. Gelation occurs when a three-dimensional network or an infinite molecular weight polymer (gel) is formed. A gel molecule cannot be dissolved in any solvent. Experimentally, gel times (the time to reach the onset of gelation at a particular temperature) are measured using rheology or solubility experiments. Free-radical crosslinking polymerization and copolymerization of multivinyl systems are very complicated and theoretical work in this field is not well established, although many papers have been published. Due to the overlap and entanglement of polymer chains, free-radical polymerizations are often diffusion-controlled even with linear chains. Crosslinking certainly confounds the diffusion-controlled reactions.

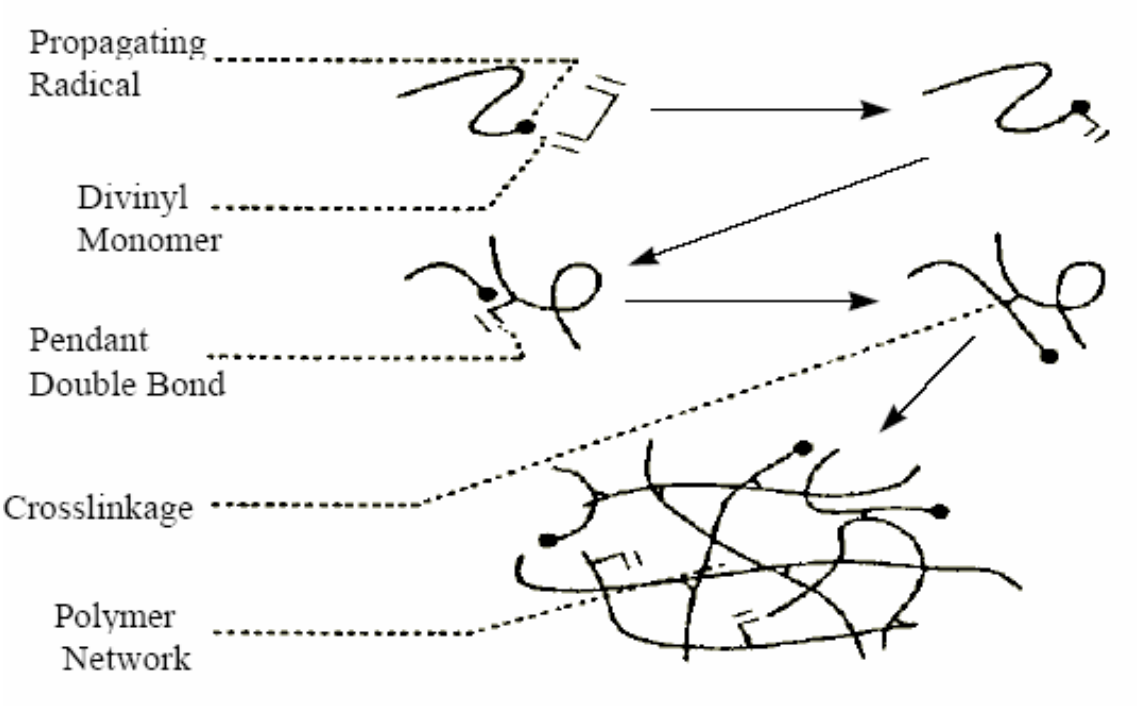

Figure 2.3. Schematic representation of free-radical crosslinking mechanism.

For the figure 2.4 shows typical temperature time relations for cross-linking of a vinyl ester following addition of initiator. The three solid curves on the right hand side of the figure

represent room temperature cross-linking of vinyl esters. The different curves illustrate different amount of initiator, inhibitor, accelerator, ambient temperature and humidity or volume of resin. A reduced amount of initiator and accelerator, as well as an increased amount of inhibitor, leads to later cross linking at lower temperature, and vice versa. The larger the volume of the resin, the faster the reaction will be. The temperature does not immediately increase after addition of an initiator despite free radicals being produced. The cross linking reaction does not start and the temperature does not increase until all inhibitor molecules have reacted with free radicals, which corresponds to inhibition time.

As cross-linking commences, the pot life is over. The resin becomes a rubbery solid quickly and the gel time is reached. The cross linking activity now accelerates very rapidly until the increasing molecular weight of the cross linking polymer starts restricting molecular movement, which occurs around the maximum temperature, and the cross linking gradually tapers off. On the other hand, the dashed line curve on the left hand side of the figure illustrates the hypothetical cross-linking as a result of the application of microwave to the resin. In this case, the inhibition time is shortened and maximum temperature is reached quickly. The maximum temperature reached is also expected to be higher. It is anticipated that the result of such a curing will reduce the shrinkage of vinyl ester because of initial uniform thermal expansion.

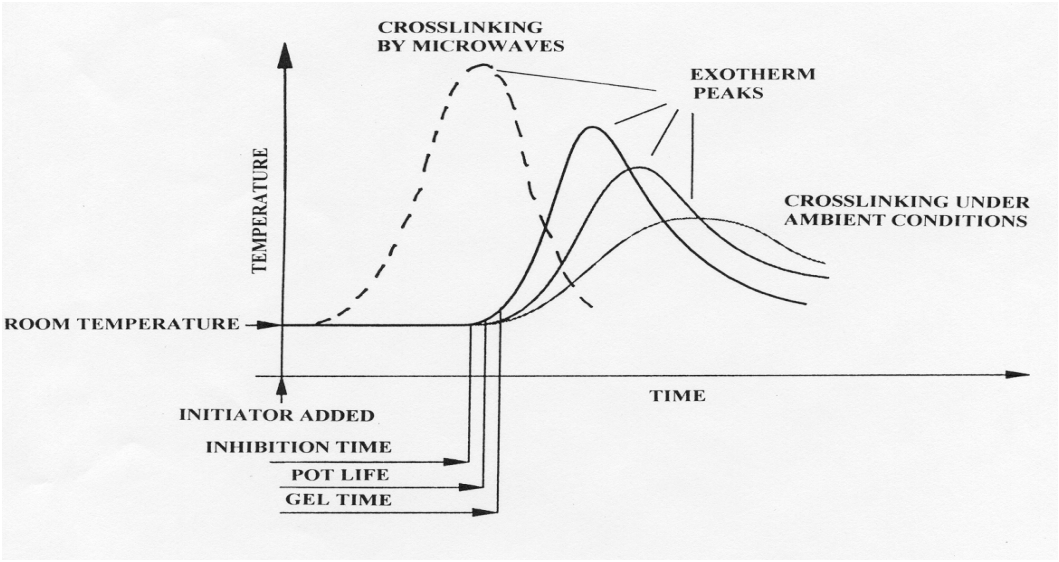

Figure 2.4: Temperature time relationships for cross linking of vinyl ester.

2.3. Introduction of Microwave

A microwave is a continuous electromagnetic spectrum that extends from low-frequency alternating currents to cosmic rays. In this continuum, the radio-frequency range is divided into bands. Bands 9, 10 and 11 constitute the microwave range that is limited on the low frequency side by Very High Frequency (VHF) and on the high-frequency side by fair infrared. These microwaves propagate through empty space at the velocity of light and their subset of radio waves and fall into the frequency range from 300 MHz to 30 GHz, as shown in figure 2.5.The VHF and ultra high frequency bands constitute a natural resource managed by three international organizations. These organizations delegate their power to national organizations for allocating frequencies to different users. Industrial microwaves are generated by a variety of devices such as magnetrons, power grid tubes, klystrons, klystrodes, crossed-field amplifiers, traveling wave tubes, and gyrotrons.

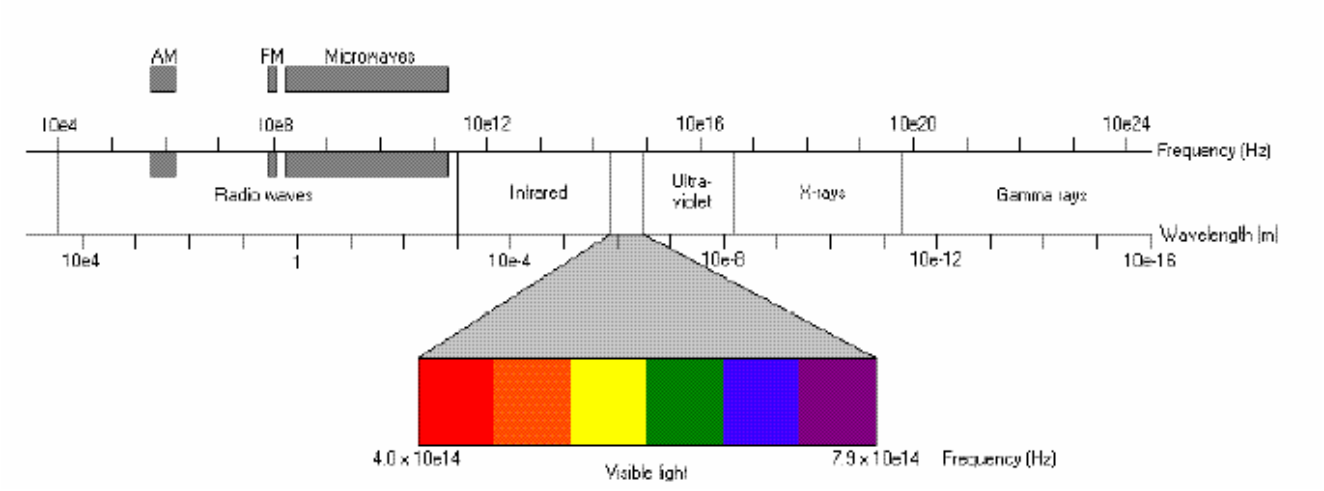

Figure 2.5: some frequency bands, exact frequencies and approximate wavelengths.

Frequency bands reserved for industrial applications are 915 MHz, 2.45GHz, 5.8GHz and 24.124 GHz. At the customary domestic microwave frequency of 2.45 GHz, the

magnetrons are the workhorse. Material processing falls into this category. The figure 2.6 shows below is the microwave oven used in the experiment.

Figure 2.6: The overview of the microwave oven

In its most familiar embodiment, shown schematically in Figure 2.7, a cylindrical electron emitter, or cathode, is surrounded by a cylindrical structure, or anode, at a high potential and containing cavities capable of supporting microwave fields. Magnets are arranged to supply a magnetic filed parallel to the axis and hence perpendicular to the anode-cathode electric field. The interaction between electrons travelling in these crossed fields and microwave fields supplied by the anode causes a net energy transfer from the applied DC voltage source to the microwave field. The interaction occurs continuously as the electrons traverse the cathode-anode region. The magnetron is the

most efficient of the microwave tubes with efficiencies up to 90 percent having been achieved (NRC, 1994).

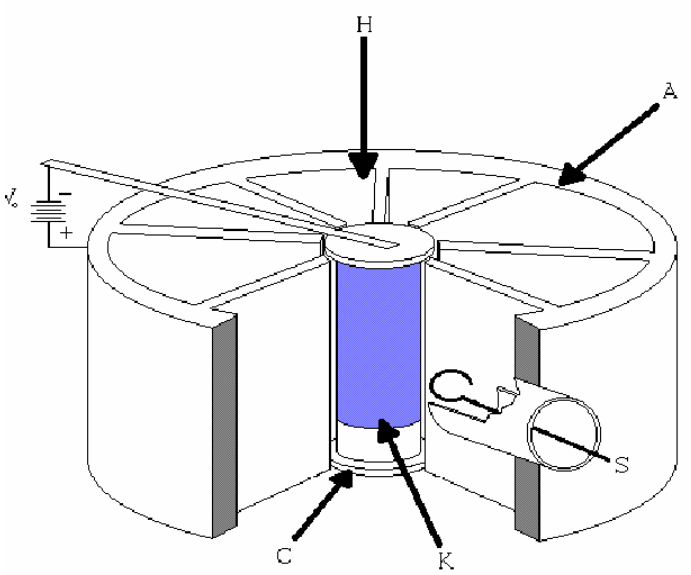

Figure 2.7: Schematic of a magnetron microwave generator

2.4. Microwave and Material Interaction

In order for a given material to be heated with microwaves, some of the energy carried in the electromagnetic field must be transferred to the material. Two fundamental properties of a material govern its interaction with electromagnetic fields in the area of microwave heating. The first of these is the dielectric constant, ε', also known as the real permittivity of the material. This property is a characterization of the ability for electromagnetic energy to penetrate the material. For most materials, this value can realistically be treated as a constant with minimal variation due to the temperature of the material and the frequency of the electromagnetic radiation. The second fundamental material property is the dielectric loss factor, ε'', also known as the dielectric loss or imaginary permittivity. It is essentially a measure of the ability of the material to store electromagnetic energy. A material with a high dielectric loss does not store the energy effectively, and a significant portion of the energy is converted ("lost") to thermal energy within the material. All of the various mechanisms that result in electromagnetic energy being dissipated in a material are included in the dielectric loss factor. The two permittivity values are often lumped together into a single parameter called the complex permittivity, εc, comprised of the real and imaginary permittivity such that:

$$\varepsilon c = \varepsilon o(\varepsilon' - j\varepsilon'') \qquad \textit{(Eqn 2.4.1)}$$

Of the two dielectric properties, the loss factor is the primary indicator of how well a given material can be heated with microwave energy. A low-loss material, with a low value of ε'', is able to store electromagnetic energy well and does not absorb much of the

stored energy. In these cases, the material may be said to have a permittivity, ε, which is essentially just the real part of the complex permittivity because the imaginary part is so small as to be negligible. A lossy material, with a high value of ε'', absorbs a larger portion of the electromagnetic energy instead of storing it all. The absorbed energy is converted into thermal energy within the material through several dissipation mechanisms. Since these materials absorb a larger portion of any incident electromagnetic energy, they are heated more readily than a low-loss material. Lossy materials are often characterized by a quantity known as the loss tangent, tan δ, which is defined as

$$\tan \delta = \varepsilon'' / \varepsilon' . \qquad \textit{(Eqn 2.4.2)}$$

The depth is controlled by the dielectric properties. Penetration depth is defined as the depth at which approximately $\frac{1}{e}$ (36.79%) of the energy has been absorbed. It is also approximately given by:

$$D_p = \left(\frac{4.8}{f}\right)\frac{\sqrt{\varepsilon'}}{\varepsilon''} \qquad \text{(Eqn 2.4.3)}$$

where D_p is in cm, f is in GHz and ε' is the dielectric constant.

Note that ε′ and ε″ can be dependent on both temperature and frequency, the extent of which depends on the materials. The results of microwaves/materials interactions are shown in figure 2.8.

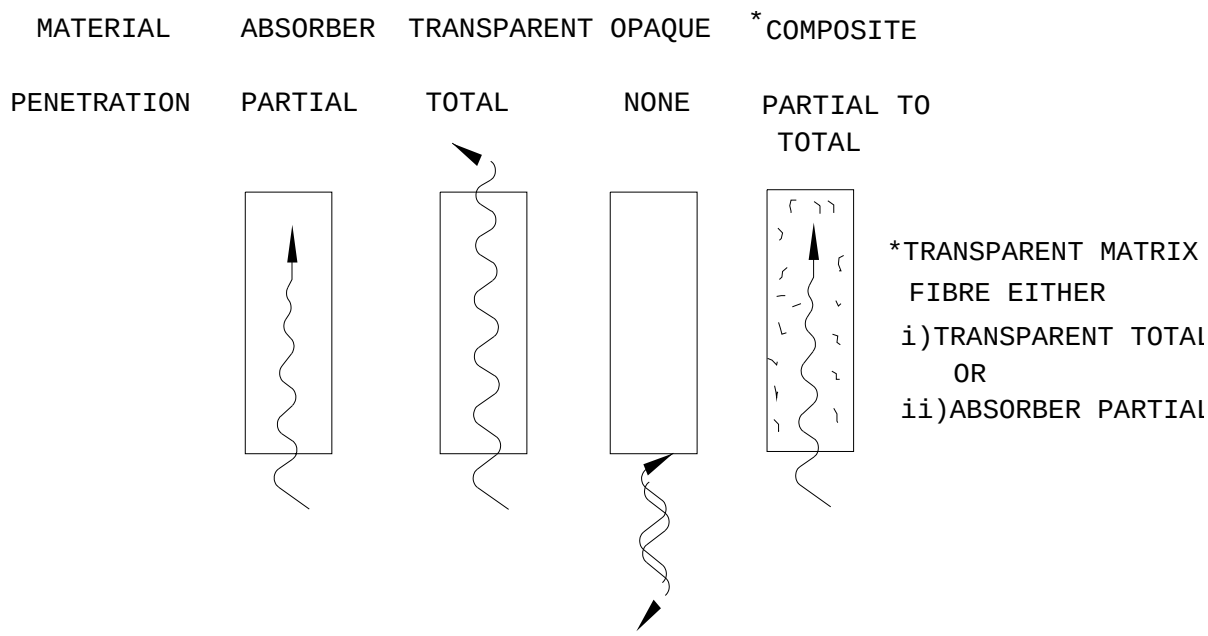

Figure 2.8: Interaction of microwaves with materials

2.4 Risks of Styrene

In this project, the resins had used 50% by weight of styrene. Styrene is volatile and evaporates easily and becomes an inhalation hazard. Styrene vapor causes mild, temporary irritant to eyes and respiratory tract at concentrations in the range of 20-100 parts per million (ppm). At the concentrations above 100-200 ppm, styrene is a definite irritant causing central nervous system (CNS) depression. According to Department of Consumer and Employment Protection, Government of Western Australia, at concentrations above 100 ppm, symptoms such as headache, dizziness and fatigue were reported. This government association also claimed that symptoms such as slower reaction times, reduced manual dexterity, and impaired co-ordination and balance can be

observed at the concentrations above 200 ppm Above 500 ppm it is a severe irritant. Besides, styrene is also highly flammable, high vapor concentrations may cause explosions. Since the human nose is extremely sensitive to the very characteristic styrene smell, the risk of acute styrene poisoning through inhalation is quite low; the odour threshold is approximately 0.1 ppm (Ku 2002). Long-term occupational exposure to styrene increases the frequency of chromosome damage in one type of blood cells and may possibly cause brain damage at concentrations as low as 10 ppm. The potential health effects of styrene in vinyl ester resins on human beings are (Fibre Glass Development Corporation, 2003):

- **Eye.** Exposure can cause eye irritation. Symptoms include stinging, tearing, redness and swelling.

- **Skin.** Exposure can cause skin irritation. Prolonged or repeated exposure may dry the skin. Symptoms include redness, burning, cracking, skin burns and skin damage. Although skin absorption is possible, under normal conditions of handling and use, harmful effects are not expected.

- **Breathing.** Breathing of vapour or mist is possible. Inhalation of small amounts of styrene during normal handling is not likely to cause harmful effects; inhalation of large amounts may be harmful. Symptoms usually occur at air concentrations higher than the recommended exposure limits.

- **Symptoms**. Symptoms of exposure to this material through breathing, swallowing, and/or passage of the material through the skin may include: metallic taste, stomach or intestinal upset (nausea, vomiting, diarrhea), irritation (nose, throat, airways), central nervous system (CNS) depression (dizziness, drowsiness, weakness, fatigue, nausea, headache, nconsciousness) and other CNS effects, loss of coordination, confusion and liver damage.

- **Swallowing.** Swallowing small amount during normal handling is not likely to cause harmful effects; swallowing large amount may be harmful. This material can enter the lungs during swallowing or vomiting. This result in lung inflammation and other lung injury.

2.4.1 Styrene Risks Safety Measure

In this section will discuss on the safety measures that should be undertaken by person that involves in the activity of using styrene. The MSDS of Fibre Glast Development Corporation suggested that the following first aid measures should be taken when styrene in the resin is exposed to:

- **Eyes.** If symptoms develop, immediately move individual away from exposure into fresh air. Flush eyes gently with water for at least 15 minutes while holding eyelids apart; seek immediate medical attention.

- **Swallowing.** Seek medical attention. If an individual is drowsy or un-conscious, do not give anything by mouth; place individual on the left side with a head down. Contact a physician, medical facility, or poison control centre for advice about how to induce vomiting. If possible, do not leave individual unattended.

- **Skin.** Remove contaminated clothing. Flush exposed area with large amount of water. If skin is damaged, seek immediate medical attention. If skin is not damaged and symptoms persist, seek medical attention. Launder clothing before reuse.

- **Inhalation.** If symptoms develop, move individual away from exposure into fresh air. If symptoms persist, seek medical attention. If breathing is difficult, administer oxygen. Keep the person warm and quiet; seek immediate medical attention.

- **Flash point**: 26.6 – 32.2 ^{o}C

- **Explosive limit (for component)**: Lower = 1.1 %, Upper = 6.1%.

- **Auto-ignition temperature**: No data.

- **Fire and explosion hazards**: Vapours are heavier than air and may travel along the ground or may be moved by ventilation and ignited by lights, other flames, sparks, heaters, smoking, electric motors, static discharge, or other ignition source locations

distant from material handling point. Never use welding or cutting torch on or near drum (even empty) because product (even just residue) can ignite explosively.

- **Extinguishing media**: Regular foam, water fog, carbon dioxide and dry chemical.

- **Fire fighting instructions**: Wear a self-contained breathing apparatus with a full face piece operated in the positive pressure demand mode with appropriated turn-out gear and chemical resistant personal protective equipment. Polymerisation will take place under fire conditions. If polymer-risation occurs in a closed container, there is possibility it will rupture violently.

2.5 Risks of MEKP

MEKP is a colourless solution of methyl ethyl ketone peroxide in dimethyl phthalate, with 9% active oxygen. MEKP should be stored in the original closed container in a cool place away from all sources of heat, sparks, or flames, and out of direct sunlight. MEKP also is a strong irritant. Avoid swallowing and all contact with eyes and skin. Ingestion can be fatal. The table 2.1 below is summaries the risk of MEKP:

Table 2.1: Table of MEKP possible risk and safety precautions.

MEKP — Possible Risks	
Combustion **Spontaneous decomposition**	Many formulations are readily flammable. A few, however, are an explosion risk, but only if exposed to undue heat or contamination by dirt, ash, rust, metal dust, concentrated acids, alkalis, or accelerators.
Damage to skin and eyes	Peroxy acids, hydro peroxides and ketone peroxides, in particular, are very corrosive.

MEKP — Safety Precautions	
Maintain recommended storage temperature **Store in closed, original containers**	Prevent drying out of water-dampened peroxides. Keep away from sources of ignition and heat. Avoid shock and friction. No Smoking!
Avoid any contamination of peroxide **Never mix peroxide and accelerator**	Do not return left-overs into storage container. Use up peroxides at once or dispose of the rest — disposal by burning after sufficient dilution.
Wear close-fitting, enclosed eye protection **Use mechanical pipetting aids**	Never suck up liquid peroxides by mouth. Apply protective skin ointment to the hands. Wear PVC gloves and a rubber apron.

Chapter 3. Introduction of Fracture Mechanics

3.1 Description of Fracture Mechanics

The fracture mechanics defined as a field of solids mechanics that deal with the behaviour of cracked bodies subjected to stresses and strains. The aims of the fracture mechanics are to determine the severity of a pre-existing defect in term of its tendency to initiate a fracture, which would cause failure.

3.2 Fracture Toughness

The typical fracture toughness test can be performed by applying a tensile stress to a specimen prepared with a flaw of known size and geometry (figure 3.1). The stress applied to the material is increasing at the flaw, which it acts as a stress raiser. The stress intensity factor K for a simple test calculation is shown as below:

$$K=f\,\sigma\sqrt{\pi a} \qquad \text{(Eqn 3.1)}$$

Where **f** is a geometry factor for the specimen and flaw, σ is the applied stress, and ***a*** is the flaw size (as defined in figure 3.1). If the specimen is assumed to have an 'infinite' width then it calculate as $f \cong 1.0$.

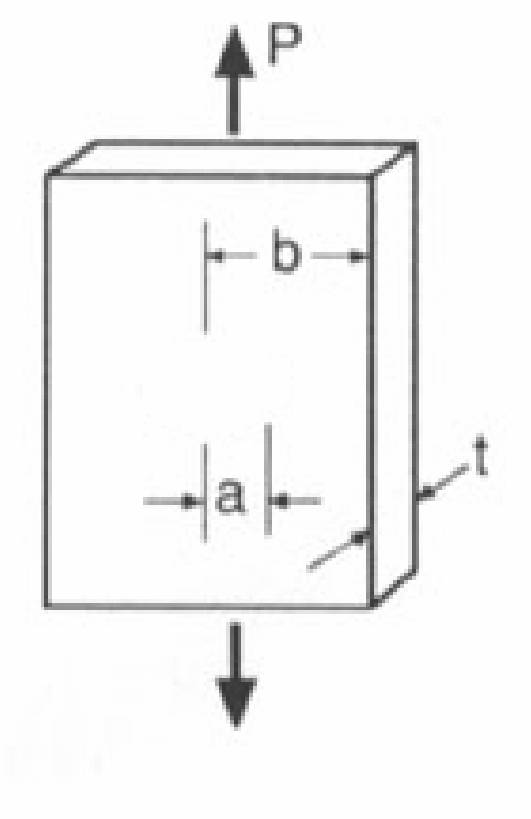

Figure 3.1: A specimen note that the entire crack length is equal to *2a.*

By performing a test on the specimen with known flaw size, the value of k that causes the flaw to grow and cause failure can be determined. The critical stress intensity factor was defined as the fracture toughness K_c is the K, which required for a crack to propagate.

Fracture toughness will depend on the thickness of the sample: this is when specimen thickness is much greater than the crack dimension. The fracture toughness K_c then will be decreased to a constant value. This constant is called the *plane strain fracture*

toughness K_{IC}. It is K_{IC} that is normally cited for most situations as the property of a material.

The critical fracture toughness value, K_{IC} can improve the reliability of a structure or component. The ability of a material to resist the growth of crack propagation based on several factors:

- **The ability of the large flaws to reduce its permitted stress**

  It can be done by using the special manufacturing techniques, such as filtering impurities from liquid metals and hot pressing of particles to produce ceramic components. It can help to reduce the flaw size and improve the fracture toughness.

- **The ability of a material to distort is critical**

  In ductile metals, the material close to the tip of the flaw can be distorted. It is causing the tip of any crack to become blunt, reducing the stress intensity factor, and preventing growth of the crack. The increasing strength of a given metal usually decreases ductility and gives lower fracture toughness. The fragile materials such as ceramics and polymers have lower fracture toughness than metals.

- **Thicker and rigid materials**

  These two kinds of materials have lower fracture toughness than thin materials.

- **Increasing the rate of application of the load**

This application as in an impact test, typically reduces the fracture toughness of the material.

- **Increasing the temperature will normally increase its fracture toughness as in the impact test**

- **A small grain size will normally improve its fracture toughness**

This is where more points are defected and dislocations reduced its fracture toughness. Hence, a fine-grained ceramic material may provide improved resistance to crack growth.

3.3 The Role of Fracture Mechanics

The roles of fracture mechanics are to design and select material that deal with the behaviour of cracked bodies subjected to stress and strains. Fracture mechanics known as a tool that will help structural engineers to a better understanding of concrete structure behaviour, a better design concrete structures and lighter concrete mixture.

There are three variables to be considered: the property of the material (K_C or K_{IC}), the stress σ that the material must withstand, and the size of the flaw *a*. Once we figure the two of these variables, the third can be determined.

The roles of fracture mechanics been explained as in several steps as below (Donald R. Askeland, 1996):

- **Selection of a material:**

  If we know the maximum size *a* of flaws in the material and the magnitude of the applied stress, we can still choose a material that has a fracture toughness K_C or K_{IC} large enough to prevent the flaw from growing.

- **Design of a component:**

  If we know the maximum size of any flaw and the material (and therefore its K_C or K_{IC}) has already been selected, we can calculate the maximum stress that the component can withstand. Then we can design the appropriate size of the part to ensure that the maximum stress is not exceeded.

- **Design of a manufacturing or testing method:**

  If the material has been selected, the applied stress is known, and the size of the component is fixed, we can calculate its fracture toughness

3.4 Theories of Mechanics and Fracture Toughness

Modifications to Griffith's theory have led to the development of the field of fracture mechanics. Fracture mechanics deals with facture initiation and crack propagation, and provides quantitative methods for characterizing the behavior of an intact material as it fractures due to crack growth. The extension of fracture mechanics to rock is understandable since rock masses contain cracks and discontinuities. States of stress around these flaws cannot be predicted using macroscopic failure criteria (i.e. Mohr-Coulomb, ultimate strength theories). In order to deal with crack propagation, particularly in terms of "intentional" fracturing as in size reduction processes, fracture mechanics must be used.

Although fracture mechanics has an undeniable place in mechanics applications, it was not developed for geomaterials. It should be recognized that differences exist between fracture mechanics for man-made materials (metals) and rock fracture mechanics, particularly in basic material response and engineering application. Whittaker (et al., 1992) gave a comprehensive list and explanation of these differences, which can be summarized as:

1. Stress state – Many rocks structures are subjected to compressive stresses as opposed to tensile stresses. However, in comminution and crushing the induced stress state is tensile (from point-load compression) and thus tensile fracture is seen in rock.

2. Rock fracture – Rock materials usually fracture in a brittle or quasi-brittle manner and usually do not exhibit plastic flow.

3. Fracture process zone (FPZ) – Non-elastic behavior ahead of a crack tip in rock takes the form of micro-cracking as opposed to excessive shear stresses and the resultant plastic process zone seen in metals. If the size of the FPZ is small then linear elastic fracture mechanics applies.

4. Crack surface – Crack surfaces in rock can be non-planar with friction and inter-locking occurring, but linear elastic fracture mechanics assumes that no forces are transmitted across the surface of a smooth planar crack

5. Crack propagation – In rocks there is a tendency for crack propagation to "wander" along grain boundaries or planes of weakness. The area of newly created surface is then larger then the assumed fracture area.

6. Rock fracture mechanics applications – In rock mechanics, as in (man-made) materials engineering, the prevention of failure by fracture growth is a concern. But the optimizing the generation and propagation of cracks is also a concern as in size reduction processes. Thus the application dictates how material parameters should be determined and used.

7. Influence of scale – Due to the complicated geologic nature of rock masses, the characterization of a rock mass is high. For the prevention of crack growth and failure, parameters measured experimentally are of secondary importance but for rock fragmentation applications, experimentally measured properties are of primary importance.

8. Heterogeneity – Changes in local structure and strength ahead of a crack tip affects the continuity of crack growth.

9. Presence of discontinuities – Pre-existing discontinuities affect the local stress states and crack propagation.

10. Anisotropy – Rocks can be anisotropic affecting measured fracture parameters as a function of crack orientation.

Recognition of these variations has led to more practical and developed concepts of fracture mechanics as it applies to behavior, with principles of linear elastic fracture

mechanics being extended even to rocks that behave non-linearly and much of the focus centering on the measurement of fracture toughness.

The most fundamental aspect of rock fracture mechanics is the establishment of a relationship between rock fracture strength and the geometry of the flaws that result in fracture. Through this relationship an intrinsic material property that describes a materials' resistance to crack propagation can be measured. This property is called fracture toughness. The application of fracture toughness in size reduction processes is clear. Fracture toughness represents a critical level above which crack extension and fracture occurs. When individual rock particles are subjected to the applied forces of size reduction, it is most likely that the intrinsic tensile property measured as the fracture toughness will control breakage (Bearman, 1998). Since the amount of energy input into a size reduction process and the amount of size reduction achieved (i.e., the fractured size distribution) are related to the type of loading and the crack pattern in the material, there should be a relationship between these parameters and fracture toughness.

3.5 Transition Temperature Approach

The transition temperature approach assumes that every material below a certain temperature will become brittle. This is caused by the material not being able to plastically yield so that the stress concentration at the crack tip can not be absorbed thus causing it to fracture a lower stress (Figure 3.2).

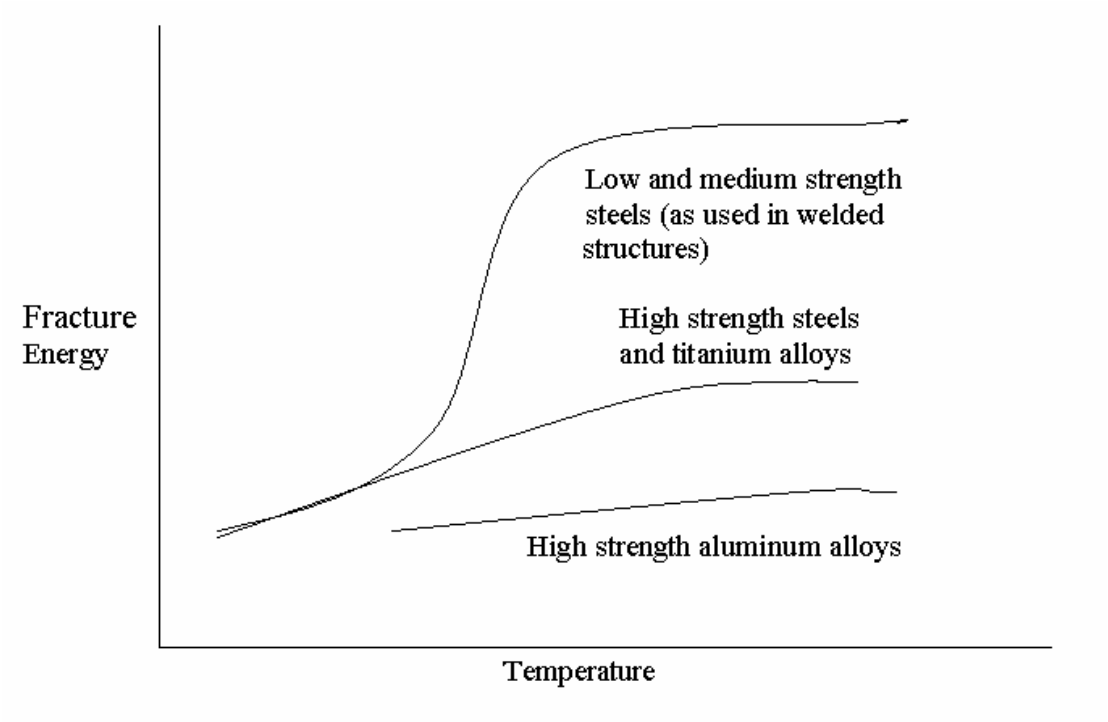

Figure 3.2: The general effect of temperature of the fracture resistance of structural metal.

Various tests are used to determine the transition temperature of a material .The transition temperature is difficult to accurately find so a range of temperatures are used, this range of results are grouped into general categories (Osgood, 1971):

- *Tougness-Frangile Transition Temperature:*

  At this point the capability of the material to with stand gross plastic deformation reduced to near zero.

- *Fracture-mode Transition Temperature:*

  At this point the crack propagates changes with decreasing temperature from full shear to flat fracture surface.

- *Fracture-stress Transition temperature:*

At this point the fracture strength of sharp- notched specimen decreases rapidly well below the yield strength.

- *Crack-Arrest Transition Temperature:*

Below this temperature, a running crack cannot be stopped.

The charpy V-notch test is often used to find the transition temperatures because several temperatures can be determined off the same from Figure 3.3.

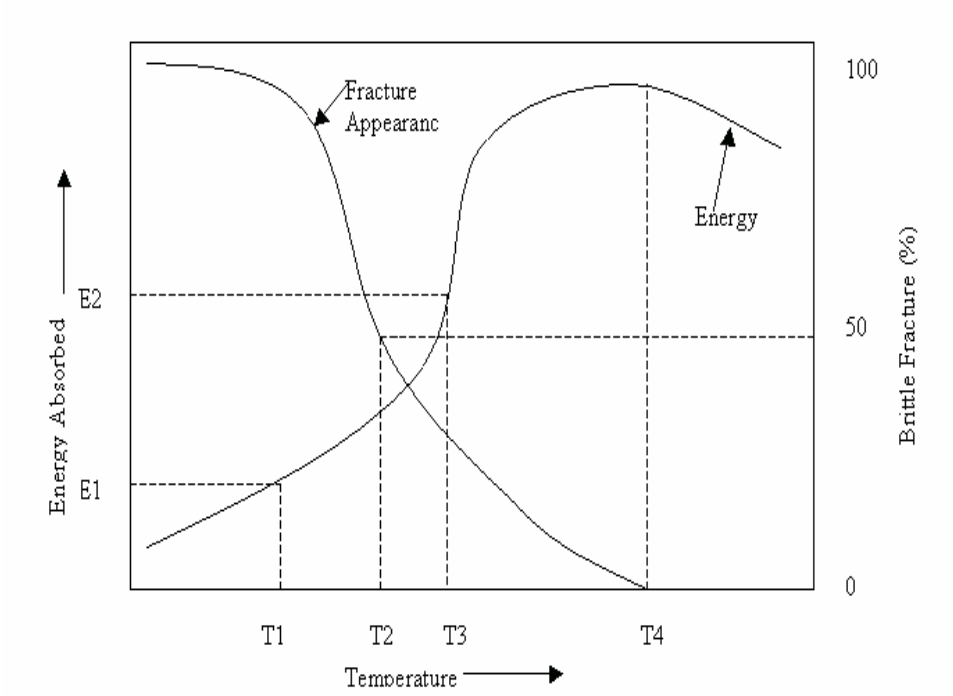

Figure 3.3: Results from Charpy V-notch impact test.

T_1 – From fixed level of impact energy

T_2 - Fracture resistance

T_3 – Midpoint temperature

T_4 – Fracture entirely sheer

The transition temperatures are compared with fracture resistance of other materials, which are considered for the design. The material with the lowest transition temperature is considered to be the most fracture resistant.

This method is determining fracture resistance, the results cannot be expressed directly in terms of load-carrying term but with use of a fracture analysis diagram (figure3.4) applied stress, defect size and temperature can be related.

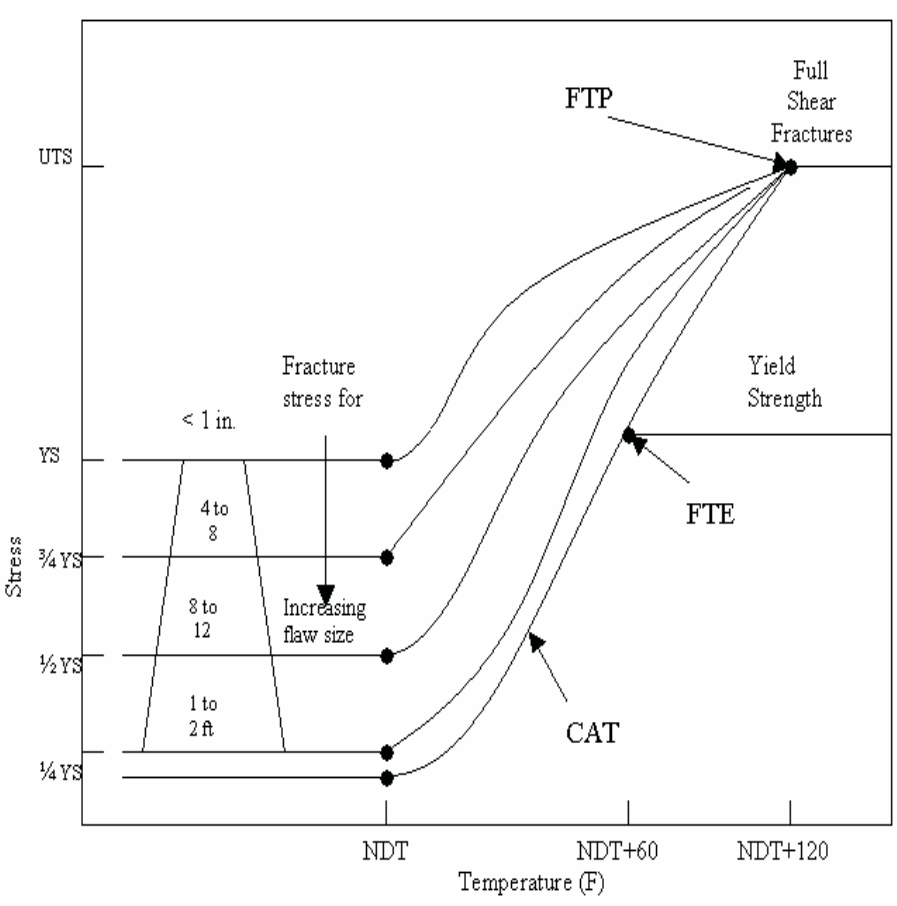

Figure 3.4: Fracture analysis diagram.

3.6 Linear Elastic Fracture Mechanics

$$2'_s aE\sigma\pi=\gamma \qquad \text{(Eqn 3.2)}$$

.

As above equation was presented as a size independent expression characterizing the resistance of a material to fracture based on the stresses required for breakage and the presence of flaws. It showed that fracture initiation in a brittle solid is controlled by the product of a far-applied stress and the square root of the flaw length which reaches a critical value determined by the characteristic material properties E, ν, and γ_s. This critical value is called the critical stress intensity factor and is denoted K_c. Irwin (1957) used a stress intensity approach to relate the critical strain energy release rate G_c to the critical stress intensity factor K_c. Rather than follow Griffith's global approach, Irwin

considered the crack tip region, which is small compared to the rest of the body but large enough with respect to atomic dimensions such that linear elastic theory applies (Knott, 1972). Irwin determined the work required to close up a small portion of a crack by superimposing tensile forces along the crack surfaces and hypothesized that this work is equal to the energy released when the crack extends. Thus the work required to close a unit length of the crack is the strain energy release rate and, based on the stresses and displacements occurring as a result of the tensile forces, is equal to:

$$G = \frac{\left(1-\nu^2\right)K^2}{E} \qquad \text{(Eqn 3.3)}$$

Since crack propagation occurs when G reaches a critical value, the critical value of stress intensity can be defined as:

$$K_c = \sqrt{\frac{G_c E}{\left(1-\nu^2\right)}} \qquad \text{(Eqn 3.4)}$$

By demonstrating the equivalence of K and G, Irwin provided the basis for the development of Linear Elastic Fracture Mechanics (LEFM). In LEFM the crack tip stresses, strains, and displacements can be characterized by K as long as inelastic yielding ahead of the crack tip is small. The advantage of LEFM is that it provides a universal approach for determining a material's resistance to fracture, as defined by K_c. As long as an explicit function for the stress intensity near a crack tip is known for a given crack geometry and loading configuration, K_c can be measured experimentally.

3.7 Stress Intensity Factor

The stress intensity factor *K*, alluded to in the previous section, characterizes the severity of the crack condition as affected by crack dimension, stress, and geometry (Dowling, 1999). Determining *K* is based on a linear-elastic approach (hence LEFM), which assumes the material in which the crack is located is isotropic and behaves according to Hooke's Law.

Different loading configurations at a crack tip lead to different modes of crack tip displacement. The different types of crack deformation are generalized using three basic modes. Mode I is the opening mode due to tension, where the crack surfaces move directly apart; Mode II is the sliding mode due to shearing, where the crack surfaces move over one another in a direction perpendicular to the crack front; Mode III is the tearing mode also due to shearing, where the crack surfaces sliding over one another but in a direction parallel to the crack front. The three basic modes can also occur in combination as "mixed-mode" loading with the superposition of the modes sufficient to describe most general three-dimensional cases of local crack tip stress and deformation fields (Tada et al., 2000). Mode I is the most commonly encountered mode in engineering applications and is also the easiest to analyze, produce experimentally on laboratory specimens, and apply (Schmidt and Rossmanith, 1983).

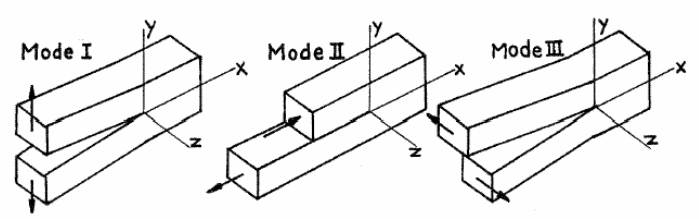

Figure 3.5: The three basic modes of crack surface displacement (*After Tada et al., 2000*)

Using theory of elasticity, namely the stress analysis methods of Muskhelishvili (1963) and Westergaard (1939), the crack tip stress and displacement fields (and hence *K*) for each mode of loading can be determined (for a complete derivation see Pook, 2000). Representing the coordinate system measured from the leading edge of a crack, the Mode I stress components are given according to the following equations 3.5:

$$\sigma_x = \frac{K_I}{\sqrt{2\pi r}}\cos\frac{\theta}{2}\left[1-\sin\frac{\theta}{2}\sin\frac{3\theta}{2}\right]$$

$$\sigma_y = \frac{K_I}{\sqrt{2\pi r}}\cos\frac{\theta}{2}\left[1+\sin\frac{\theta}{2}\sin\frac{3\theta}{2}\right]$$

$$\tau_{xy} = \frac{K_I}{\sqrt{2\pi r}}\cos\frac{\theta}{2}\left[\sin\frac{\theta}{2}\cos\frac{3\theta}{2}\right]$$

$$\sigma_z = \nu\left(\sigma_x+\sigma_y\right), \text{ for plane strain}$$

$$\sigma_z = 0, \text{ for plane stress}$$

$$\tau_{xz} = \tau_{yz} = 0$$

(Eqn 3.5)

where K_I is the stress intensity factor for Mode I. The displacements at the crack tip can be found by substituting above equation into Hooke's Law.

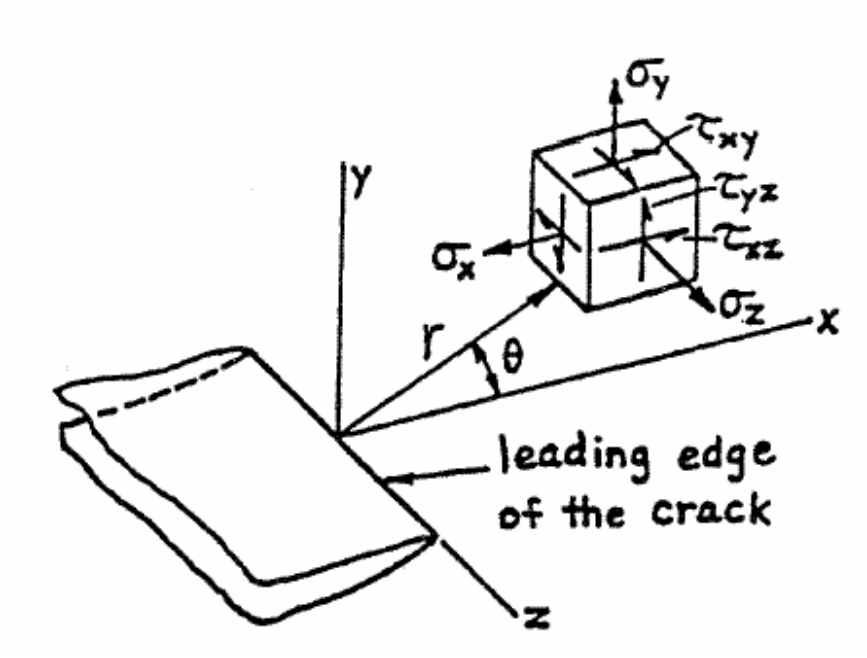

Figure 3.6 Coordinate system for a crack tip

It can be seen from Equations 3.5 that at the crack tip (as r approaches zero) the stresses approach infinity, as has already been indicated by Inglis' solution for stresses around an elliptical hole in a stressed plate. Since no value of stress at the crack tip can be given, and all non-zero stresses of Equation 3.5 are proportional to K_I, with the remaining factors varying only with r and θ, the stress field near the crack tip can be determined by giving the value of K_I, which has a formal definition of (Dowling, 1999; Pook, 2000):

$$K_I = \lim_{r,\theta \to 0} \sigma_y \sqrt{2\pi r} \quad \text{(Eqn 3.6)}$$

It was noted earlier that K_I is affected by the crack size, stress, and geometry. In order to account for different geometries Equation 3.6 can be rewritten as:

$$K_I = F\sigma\sqrt{2\pi a} \quad \text{(Eqn 3.7)}$$

where, *F* is a dimensionless constant dependent on the geometric configuration

σ is the stress averaged over the gross area *a* is the half-crack length. *F* can generally be described as a function of loading geometry and *aw* where *w* is defined as the maximum possible crack length. When *F* is determined for a given geometry the critical value of stress intensity, or fracture toughness, can be determined as long as inelastic yielding ahead of the crack tip is small and the conditions for LEFM are met. Equations and values of *F* for a wide range of crack, specimen, and loading geometries are determined using analytical, numerical, and experimental methods and have been compiled in various handbooks (see Tada et al., 2000; Murakami, 1987; Rooke and Cartwright, 1976; Sih, 1973).

Chapter 4. Fracture Toughness Tests

4.1 Description of Fracture Toughness Tests

The K_{IC} is an extremely important property in many crucial design applications. The K_{IC} is a material of a sharp crack that has the characteristics of its resistance to fracture under tensile conditions.

When the stress intensity factor grows and becomes higher than K_{IC} the crack will automatically become unstable and it will propagate quickly until fracture occurs.

The material usually fails in a brittle manner when it is in plane strain conditions. *Plane strain* is the term when the stress state is characterized with thick or bulky parts for which the stress of the flaw is in triaxial tension. In plane strain conditions, if the stress intensity factor exceeds its critical value, the flaw will propagate unexpectedly and run completely through the section.

The plane stress condition is related to all sections of two-dimensional parts. This is where the most complicated stress can occur and known as biaxial. In parts, those in plane stress the flaw will grow slowly until it is below the increased stress. The flaw will then propagate unexpectedly and total fracture occurs.

The basic concepts of crack growth explain why the plane strain leads to rapid fracture and why the plane stress leads to slow fracture. Hence, it is the reason that the

plane strain fracture toughness K_{IC} is known as such an important property in fracture prevention.

There are several kinds of different testing methods that can be used to determine the fracture toughness, K_{IC}. The following sections will briefly explain some of the standard and non-standard testing procedures.

4.2 Standard Test Methods

The famous two countries named as: United States of America (USA) and United Kingdom (UK) have adopted two similar testing procedures for determining K_{IC}. These tests are documented in The American Standard ASTM: E339 and the British Standard BS: 5447. All of the standard tests have their own nominal dimensions for various specimens recommended by the respective standards. All of the specimens have own single edge notches that are initiated by low stress fatigue cracking.

4.2.1 Compact Tensile Specimen

The compact tension is a flat plate with single notch, which is fatigue cracked (Figure 4.1). The load is applied throughout two pins in line with the crack tip. As the result, this causes the two-point load onto the specimen.

Figure 4.1: Compact tensile specimen.

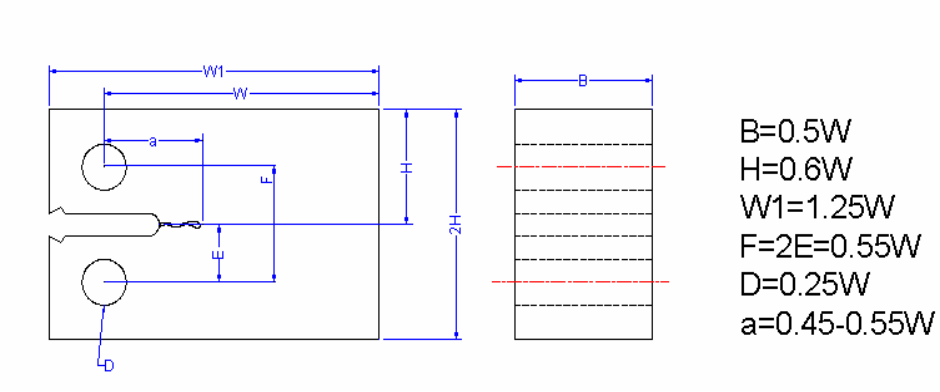

4.2.2 C-Shape Specimen

The purpose of C-shaped specimens is to check on portions of hollow cylinders. The C-shaped specimens have a single notch mid-center of arc which is fatigue cracked. The specimen is loaded throughout pins in two-point bending (Figure4.2.).

Figure 4.2: The C-shape specimen.

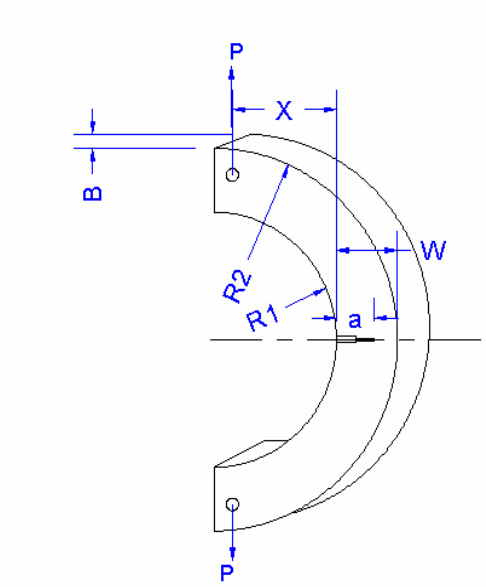

4.3 Non-Standard Test Methods

There are other kinds of tests, which are considered as non-standard tests. The data from these tests described as the mechanical properties of the material. These mechanical properties are related to the fracture toughness. The tests were developed due to its high cost and its inconvenient size of the samples required in the standard tests.

4.3.1 Charpy V-Notch Test

Figure 4.3: Charpy V-notch test rig and sample.

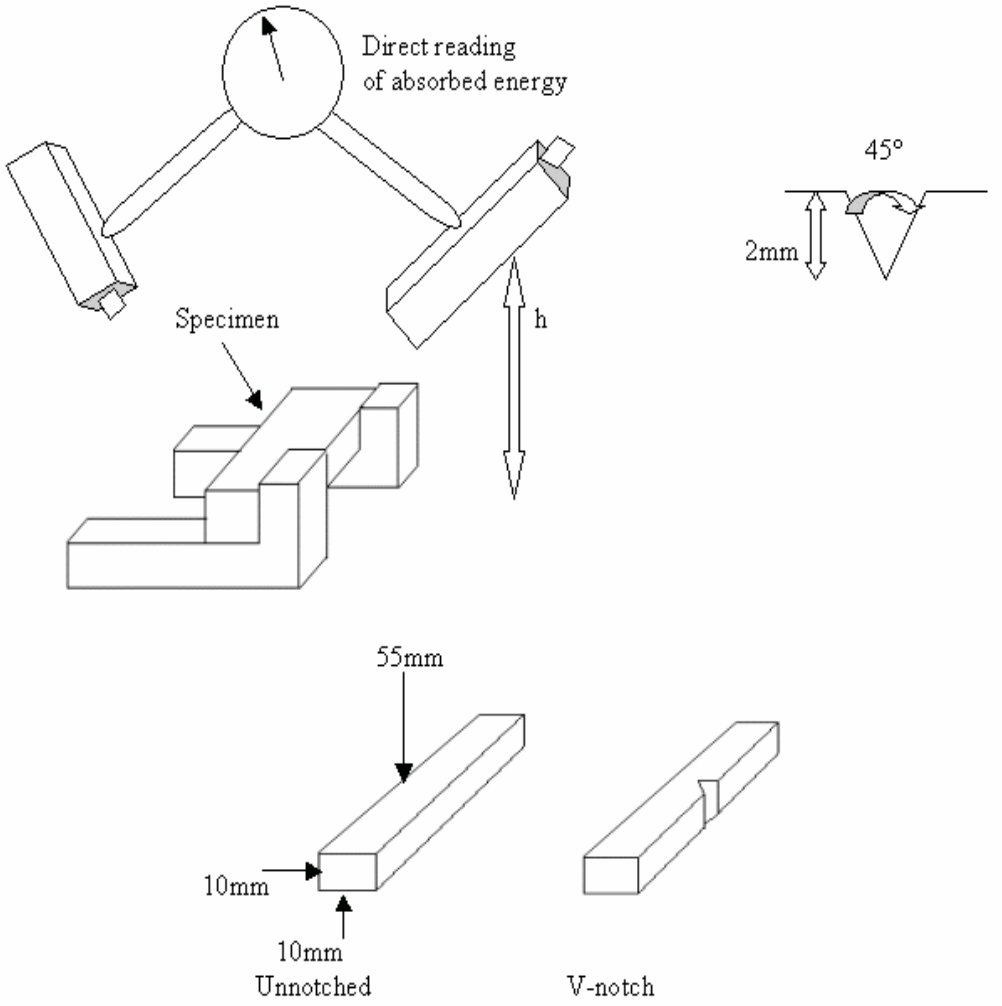

The Charpy V-notch test (Figure4.3.) is used to determine the resistance of the material to crack propagation. In this test, the impact energies are measured with reverence to the temperature. The following two equations can be used to relate the impact test to fracture toughness in order to determine the K_{IC} value of a material:

$$K_{IC}^{2} = 2\,E\,(CVN)^{3/2} \qquad \text{(Eqn 4.3.1.2)}$$

$$K_{IC}^{2} = 8\,E\,(CVN) \qquad \text{(Eqn 4.3.1.3)}$$

The Charpy V-Notch (C_v-NDT) test is associated to the impact energy $C_{v.}$ that is also associated to the nil-ductility transition temperature. The C_v energy does not correspond directly to the NDT level of fracture resistance. This make the value of C_v is unique for each type of steel; a correlation value should always be used. The V-notch impact test values are generally suitable for correlation with fracture toughness values.

4.3.2 Short Bar Test

Barker (1977) started to work on the concept of devising a simplified method to measure plane strain fracture toughness. The simplified method used small rod and bar shape specimens, that will be cracked fracjack mechanism or by other test rigs. The test is started with an opening load (F) applied to the mouth of the specimen. This causes a fracture to initiate at the point of the chevron. The constant widening of the crack front, as it evolved along the axis of the specimen can causes stable crack

growth, even in brittle materials. Hence, a "real" crack is created in the specimen before the toughness measurement is made.

For Linear Elastic Fracture Mechanics (LEFM) materials, the fracture toughness measurement is made at the time of maximum load. It is made when the crack is in the central region (critical crack length) of the specimen. For additional ductile materials, specimen mouth opening displacement is recorded as a function of opening load and simple data analysis methods allocate the calculation of K_{IcSR} (Plane Strain Fracture Toughness, as measured by the Chevron-Notched Short Rod Method).

The load-displacement data allows correction for effects caused by residual stresses in the specimen or plasticity effects in the crack growth. Data analysis methods use to analyze the crack-jump as well as smooth-crack growth types of materials.

The advantages of using short bar test are that the samples size is smaller and it is cheaper to make and to test. The requirement of E 399 for fatigue pre-cracking is not required because of the chevron shaped cut and the short test will be discussed in details in chapter 5.

Figure 4.4: Short rod specimen configuration and dimensions.

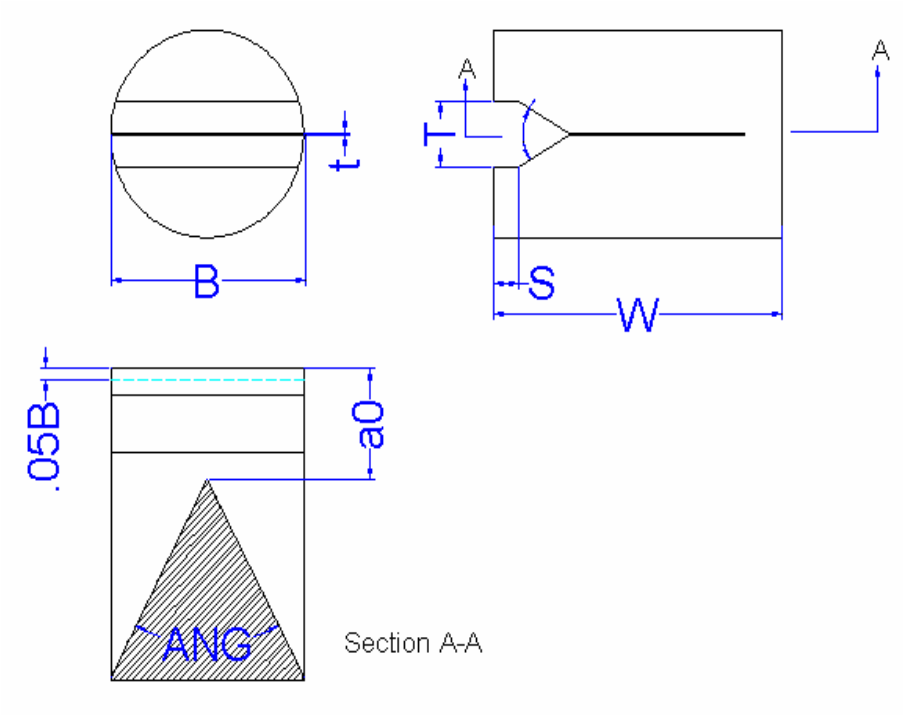

4.4 Analysis of Fracture

Figure 4.5: The instruments magnification ranges.

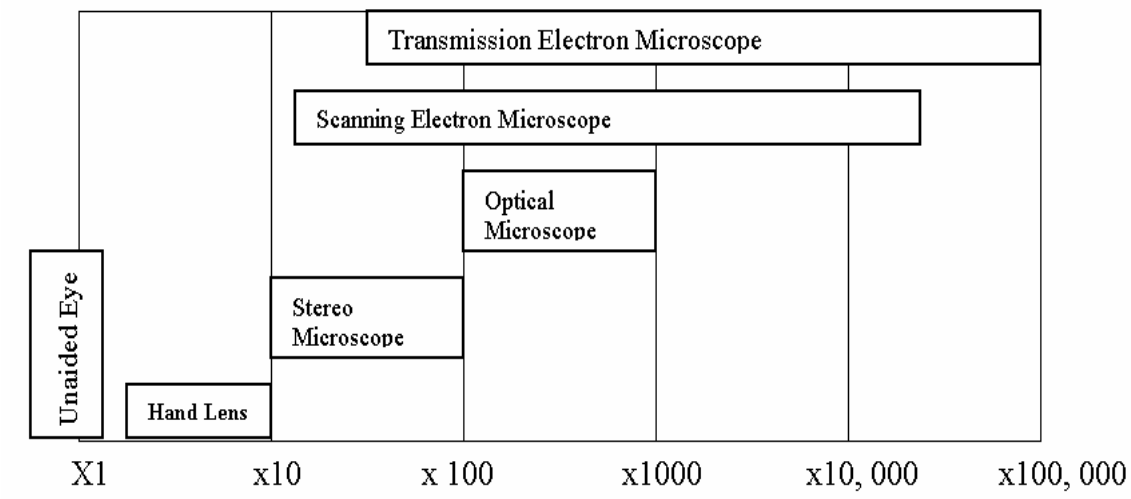

Fractured surfaces show both macroscopic and microscopic features, where a wide range of instruments with varying magnifications are required. Figure 4.5 shows the magnification ranges, which the certain instruments are effective.

Macroscopic test of the fractured surface have to be completed first, as this can be done with the naked eye or a hand lens. This usually indicates the crack origins and the direction of crack growth. In recent failures, the mode of failure can sometimes be distinguished as the surface has not begun to corrode.

When the site of the crack nucleation is identified, a stereomicroscope is the most useful tool to examine the crack origin for notable features as this could assist in the determination of the mode of fracture.

The Scanning Electron Microscope (SEM) is a very useful tool to examine the fracture surfaces. The advantages of this SEM is because it has a large depth of field and has a wide range of working magnification from low to high magnifications. The SEM has virtually replaced the optical microscope for direct examination of fractured surfaces.

The Transmission Electron Microscope (TEM) is very useful tool in the field of fractography due to its fracture surface details that can be studied at very high magnifications (up to x100, 000). There are two disadvantages of TEM; it is time consuming and it needs required skills to prepare samples that would be useful.

4.4.1 Brittle Fracture

Brittle fractures generally occur with slight plastic deformation. The strain rates within the material are regularly high because of the stress systems. Brittle fractures occur with little warning because the crack knows how to grow at the speed of sound. Excessive overloading or an impact force can cause a brittle fracture.

Macroscopic analysis of a brittle material failure shows that the materials fail differently which depends on whether it was in tension or compression. When the material fails in tension, the crack is perpendicular to the applied load. If the sample fails in compression the fracture will occur at 45 degrees to the applied load.

The crack is usually initiated from flaws of the material; these can be caused by either surface finish or impurities within the material. The cracks can be intergranular or transgranular depending on the material. A truly brittle fracture is caused by cleavage, which mean transgranular. Cleavage occurs when the material is under high constraint conditions (Baddeley, D T and Ballard J, 1991).

4.4.2 Ductile Fracture

A ductile fracture is the cresult of plastic deformation prior to failure. A ductile fracture usually occurs when the sample is in strain. Overloading usually causes ductile transgranular fractures. It can be sometimes recognized from macroscopic test of the failed specimen. Usually the specimen is thin size and there is contraction of the sample before failure occurs.

At a microscopic level, most of the structural materials fail by a process called microvoid coalescence. Microvoid coalescence caused the fractured surface to have a dimple appearance with both large and small dimples. The shape of the dimple is influenced by the type of loading which is applied to the sample. Failures caused by shear will produce extended shaped dimples that point in the opposite directions on the matching fracture surfaces. Tensile tearing produces extended dimples that point in the same direction on matching fracture surfaces (Baddeley, D T and Ballard J, 1991).

Chapter 5. Short Bar Test

5.1 Standard Tests

United and the United Kingdom have adopted two similar testing procedures for determining Kic. These tests are documented in the Standard Test Method (ASTM) and the British Standards Institution Test Method (BS).
All standard tests have there nominal dimensions for the various specimens recommend by there respective standards. All the specimens have a single edge notches that ate initiated by low stress fatigue cracking.

5.2 Non Standard Tests

There are other tests that are considered as non-standard tests, such as Charpy V-notch test and Short rod/ bar test. The data from these tests which describe the mechanical properties of the material and then be related to the fracture toughness. These test were developed because of the cost and size of the sample required in the standard test.

5.2.1 Short Bar Test

Since the fracture toughness of a material is an important property, which is crucial in design applications. Using ASTM and BS standard tests can only obtain a valid measurement of Kic; however these standards have many disadvantages such as:

- The size of the specimen required by the standard is too large that it precludes the fracture toughness measurement because a sufficiently large specimen cannot be removed from the structure of interest.

- With the size of specimen required, the size of tensile machine is very large which means that the availability of machine is very limited and the cost of testing is in big amount of money as well.

- Some material properties such as brittleness and high fracture toughness combined with low yield strength sometimes makes it impossible to meet the specimen requirements of the standard tests.

- The fatigue pre-cracking which is required of the samples.

- The difficulties in measuring the crack length.

- The overall cost of testing one sample is very expensive.

An alternative test method was considered, which was less complex and applicable to a wider range of materials. Barker considered that the test samples should exhibit some crack growth stability. His testing method used simple fracture toughness concepts to test sample configurations exhibiting crack growth even when loaded by a controlled force machine. Once calibrated for specimen configurations, the only parameter required for fracture toughness values was the peak force required to completely fracture the sample. This new test method used samples of a circular of

rectangular cross section, which were called short rod/bar samples accordingly (Barker, 1977).

On the other hand, the advantages of short bar test were (DiJon Inc, Technical note 503):

- No fatigue pre-cracking was required therefore the method was applicable to brittle as well as ductile materials.
- No load versus deflection graph required.
- No crack position or crack length measurements required.
- The size of specimen for a valid test has been reduced.

Therefore, those advantages are able to amount up to a reduction in costs of testing equipment and samples. Now this method is now being considered by an ASTM committee as an additional specimen configuration for the determination of fracture toughness (Kic).

5.3 Selection of The Short Rod or Bar Geometry

The configuration of the short bar specimen was selected on the basis of large number of tests of specimens with different length-to-diameter ratios and various chevron slot geometries. The criteria on which the current geometry was selected was:

- The tendency for the crack to “pop” at the initiation should be minimized. The crack initiation should be as smooth as possible.

- The crack should tend to be well guided by the chevron slot.

- The width of the crack front should be considerable portion of the specimen diameter at the time of toughness measurement.

- The crack should be near the centre of the specimen (far from both ends) at the time of the toughness measurement.

- The load should be at or near its peak value at the time of toughness measurement.

- The specimen geometry should be as simple as possible for ease of fabrication.

- The specimen should economical in its use of sample material.

Some of these criteria could not be achieved and the same time. The short rod and bar specimen configurations were selected as a reasonable compromise in an attempt for an optimum geometry. [Baker, 1981]

5.4 Geometry of Specimen

The four basic geometries are illustrated in figure 5.1. There are four different geometries, so that the mode of manufacture can differ where required. The decision on whether to use a short bar or rod specimens depends on the machining equipment available. The short rod is easier to manufacture when a lathe is available. The plan view (Section A-A) show that the short bar and rod specimens are exactly the same. The short bar and rod calibrations are the same and experimental studies have shown

that the two samples can be considered equivalent (Barker, 1979). The slots have different geometries because of the way in which the slots are cut. The straight-line slots are cut using a saw or cutter, which moves through the specimen.

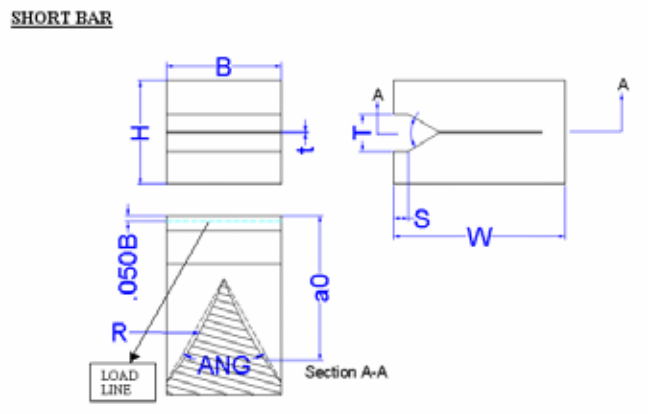

SYMBOL	DEFINITION	VALUE	TOLERANCE
B	BREADT	B	
W	LENGTH	1.5B	±.010B
H	HEIGHT	.870B	±.005B
a_0	INITIAL CRACK LENGTH	.513B	±.005B
ANG	SLOT ANGLE	55.2°	±1/2°
τ	SLOT THICKNESS	SEE FIGURE 5.5	
S	GRIP GROOVE DEPTH	.130B	±.130B
T	GRIP GROOVE WIDTH	.313B	±.313B
R	RADIUS OF SLOT CUT	SEE FIG 5.4	±2.5B

Figure 5.1: Short bar specimens with curved chevron slots.

The curved slots have different geometries because of the way in which the slots are cut. The straight line slots are cut using a saw or cutter which moves through the specimen. The cured slots are obtained using a cutter which has a plunge type feed. Since the calibration of the straight slotted specimens and the curved-slotted specimens are not equivalent.

The geometries were modified by superimposing the both the plan views and adjusting them until the slots configurations were a tangent to each other, this gave a critical crack length, a_c as shown in figure 5.2. The critical crack length is where the peak load occurs which is where the fracture toughness measurement is made. Since it is easier to measure the curved slots in terms of a_0, the distance from the edge of sample to the point of the slot, and chord angle θ (figure 5.1). A table of equivalent a_c for various a_0 and θ (figure 5.3) so that a constant specimen calibration can be used regardless of specimen size, when the crack is in the vicinity of the critical crack length, a_c.

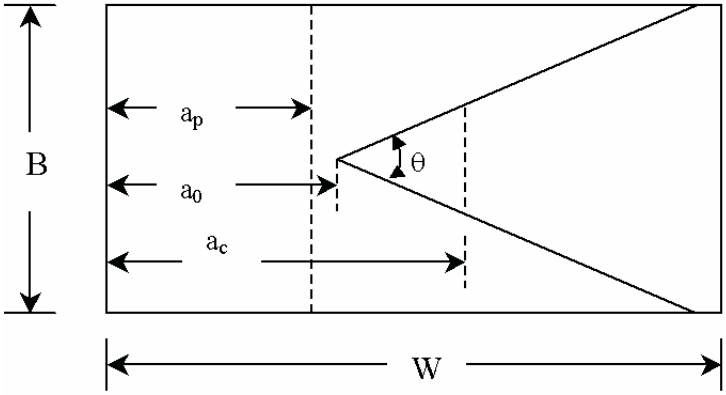

Figure 5.2: Diagram of critical crack length.

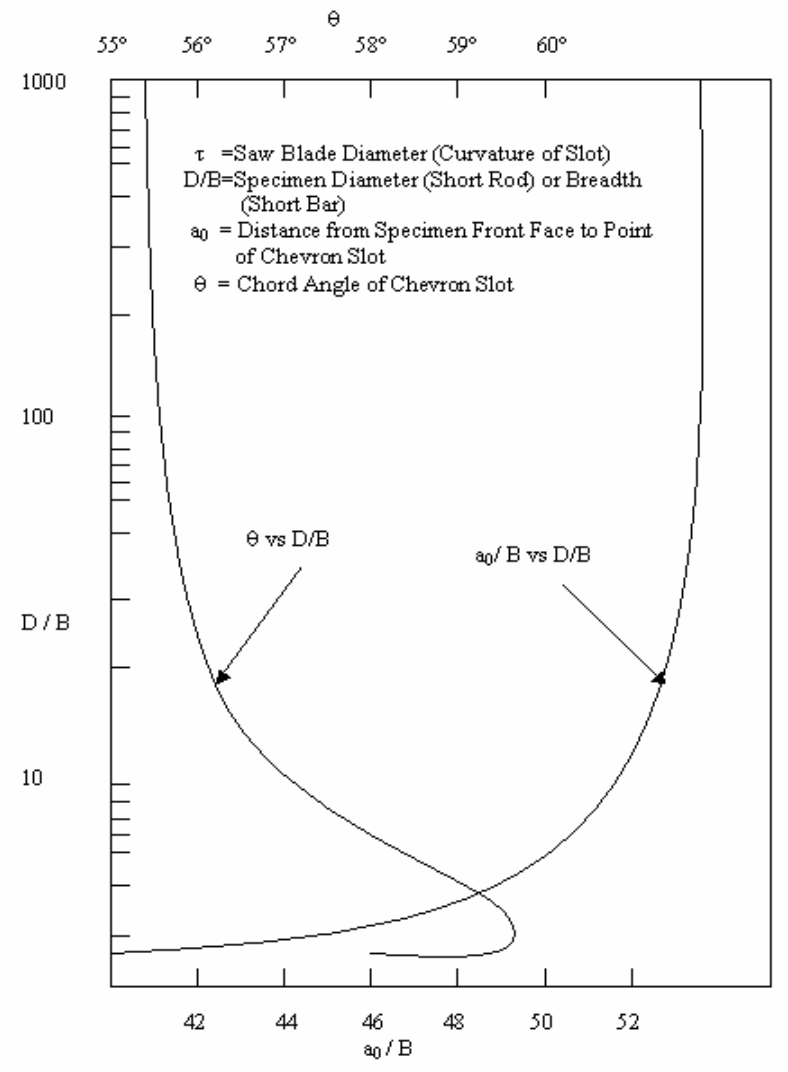

Figure 5.3: The equivalence for curved chevron slots.

Configuration correction factors were calculated because it was known how sensitive the test results were to variations in a_0, 0, W. The test results can be corrected by multiplying the results by Cc, this only works for specimens, which are out of tolerance by three times the tolerance limits.

5.5 Short Bar Test Description

With the short bar test not only are the specimen geometry and preparation important in fracture toughness results, but the testing procedure must also be controlled to obtain valid fracture toughness result.

The short bar tests involve an opening load being applied near the mouth of the specimen, causing a crack to initiate at the point of the chevron slot. Ideally, the opening load should be less than the load that will be required to further advance the crack. A continually increasing load must be supplied until the crack length reaches the critical crack length, a_c. Beyond a_c, the load should decrease, as shown in figure 5.4.

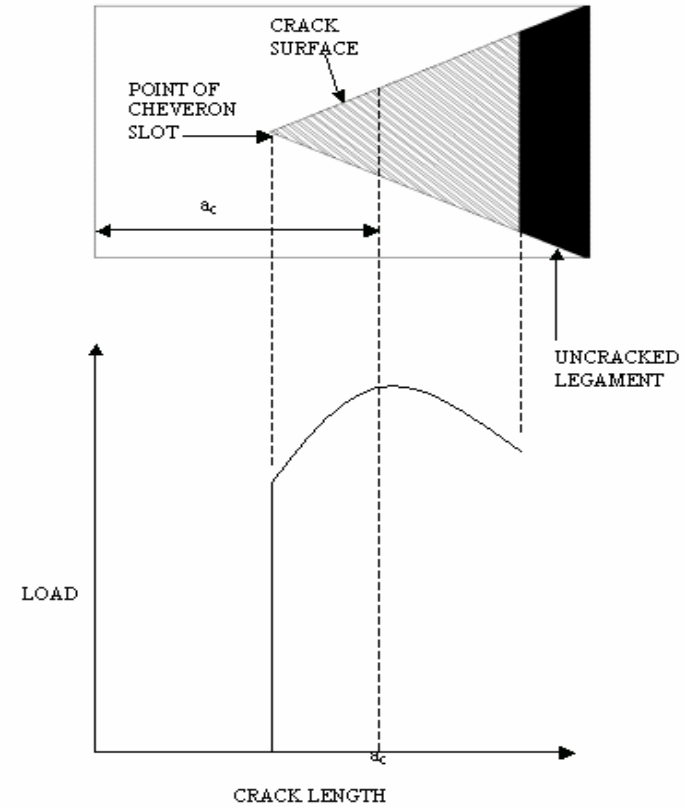

Figure 5.4 Variation of load versus crack length.

The equation for fracture toughness in a short bar test can be derived from basic fracture mechanics using the assumptions of linear elastic fracture mechanics (LEFM). K_{IC} was determined with the compact specimens using 5% secant method and the K-calibration according to ASTM E-399-78.K was calculated from the maximum load applied and the crack length including the stable crack extension.

"K_{ICSB}" of the short bar and "K_{ICSR}" of the short rod specimens were calculated from the maximum load using compliance calibration:

$$K_{ICSB} = \frac{(F_{max} Y_m^*)}{B\sqrt{W}} \qquad \text{(Eqn 5.1)}$$

With

$$Y_m^* = \{- 0.36 + 5.48\omega + 0.08\omega^2 + (30.65 - 27.49\omega + 7.46\omega)\,\alpha_0 + (65.90 + 18.44\omega - 9.76\omega)\alpha_0^2\} \left\{\frac{\alpha_1 - \alpha_0}{1 - \alpha_0}\right\}^{\frac{1}{2}} \qquad \text{(Eqn 5.2)}$$

$$K_{ICSR} = \frac{(F_{max} Y_m^*)}{B\sqrt{D}} \qquad \text{(Eqn 5.3)}$$

With

$$Y_m^* = \{19.98 - 9.54\,W/D + 6.8\,(W/D)^2 + [-118.7 + 125.1\,W/D - 22.08\,(W/D)^2]\,\alpha_0 + [379.4 - 363.3\,W/D + 84.4\,(W/D)^2]\,\alpha_0^2\} \left\{\frac{\alpha_1 - \alpha_0}{1 - \alpha_0}\right\}^{\frac{1}{2}} \qquad \text{(Eqn 5.4)}$$

Where, W = Width, H=Height, D=diameter, B=Breadth

$$\omega = \frac{W}{H}, \alpha_0 = \frac{a_0}{W}, \alpha_1 = \frac{a_1}{W}$$

Chapter 6. Experiment Method

6.1 Specimen Preparation

Initially, the dimensions of specimen are accordingly modified to the geometrical requirements for the standard ISRM short rod or bar test, where the length to diameter (short rod) or breadth (short bar) ratio, $\frac{L}{D}$ =1.45; the range of diameters can only be varied from test to test in the range of 46 – 92 mm for the tensile test. The choosing of scale is significant for the convenience of fabricating the features of the moulds. The dimension of the short bar specimen decided is attached in Appendix B.

6.2 The Process of build up the Mould

There are several criteria to preparing the moulds.

- How to recycle the experimented moulds.
- How much will the vinyl ester specimen shrinkage be.
- The cardboard strong enough to contain the heated vinyl ester composite.

Therefore we have to improve the mould. The following procedures were carried out in fabricating the moulds:

1. Drafted the part and base of the moulds.

2. Converted the draft into computer-aided drawing by using the Auto-CAD 2002 LT. as shown in the figure 6.1

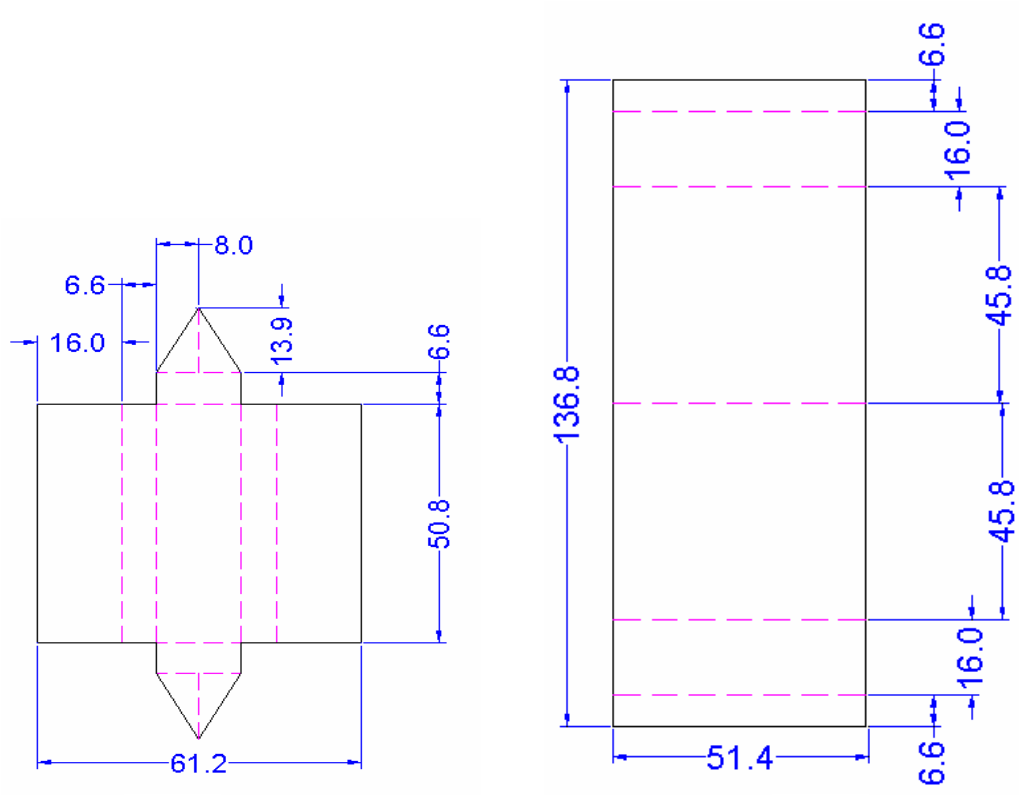

(a) (b)

Figures 6.1: The Auto-CAD drawing (a) and (b) for the triangle part of the mould.

3. The cardboard and manila folders were cut according to the figure 6.1.

4. The part being cut was folded and pasted with super glue. For the manila folder part, it looked like figure 6.2 after being folded and pasted

5. The manila folder part was pasted according to the base.

6. The internal view of the complete mould is shown in the figure 6.3.

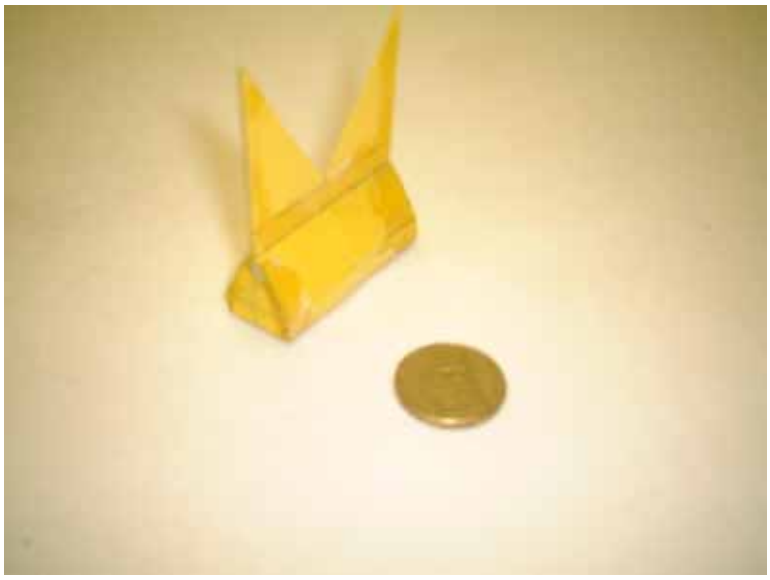

Figure 6.2: The triangle mould for making the slot and important features of short bar specimen.

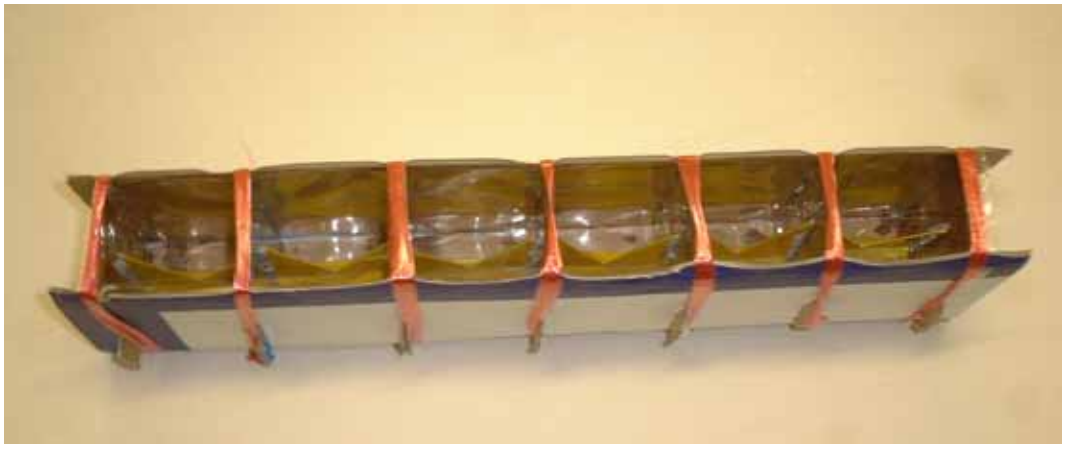

Figure 6.3: The internal view of short bar specimen mould.

In this study, I built up the mould for features of the specimen following the step as shown below:

1. First of all, building up the mould by using cardboard and seal the gap with bul-tack and super glue properly.
2. The surface of cardboard was folded with overhead projector sheet to decrease the cohesiveness of vinyl ester to the mould; the chevron slot for the sample was also made.
3. Spray the canola oil (cooking use) on the surface of the overhead projector sheet as illustrated in the figure 6.4. For pasting the triangle part, some normal glue with low bonding strength was used instead of super glue because it was found that the bonding strength would affect the results obtained.

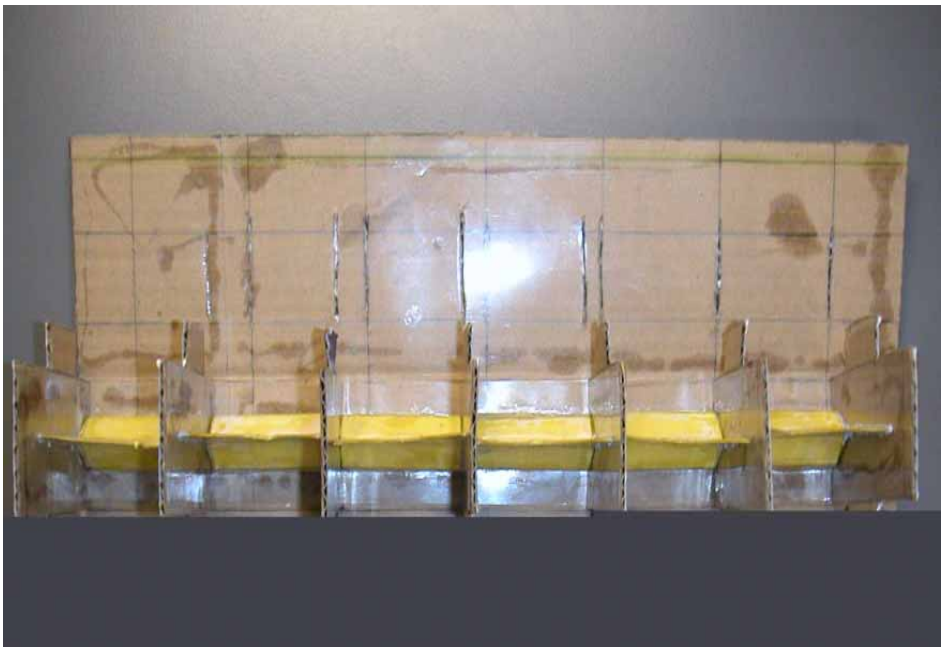

Figure 6.4: Top view of mould with canola oil and pasted with project sheet.

Figure 6.5: The super glue that I used in this study

6.3 Material Preparation Process

This is the process for preparing the specimen material:

1. Determined the amount of vinyl ester needed and the percentage by weight of fly ash in vinyl ester.
2. Calculated the amount of fly ash, accelerator and resins needed by using the ratio table shown in table 6.1.

Table 6.1: Weight of materials required to make 1230ml of VE/FLYASH(33%).

Parameters	**Resin**	**Accelerator**	**Fly ash**	**Composite**
Relative density	1.1	1.0	0.7	---
Percentage by volume	56	---	44	100
Percentage by weight	67	---	33	100
Weight for 800 ml of composite	742.54(g)	13.60(g)	378.84(g)	---

4. Poured the amount of each material according to the ratio table into different container. The weight of flyash and resins were weighted using a digital balance.

5. Poured the accelerator from its dispenser into the resins and mixed them thoroughly using a spoon.

6. Poured the fly ash into the mixture of resins and accelerator. Stir them under the exhaust fan because the styrene of the vinyl ester and the accelerator were inhalation hazardous.

7. After stirring for few minutes, poured the mixture into the mould slowly.

8. Left the material to cure under the exhaust fan or took the material for microwave exposure and cured under the exhaust fan later.

The most important things is wear the mask, goggle and gloves during the preparation processes as the styrene in the resin is inhalation hazardous and may cause problem to the skin.

6.4 Microwave Exposure of Composites

6.4.1 Modified Microwave Oven

The microwave oven was used for performing the exposure, which microwave oven did a little modified. The main part is to direct the rapid exhaust for the styrene gas, which is poisoning.

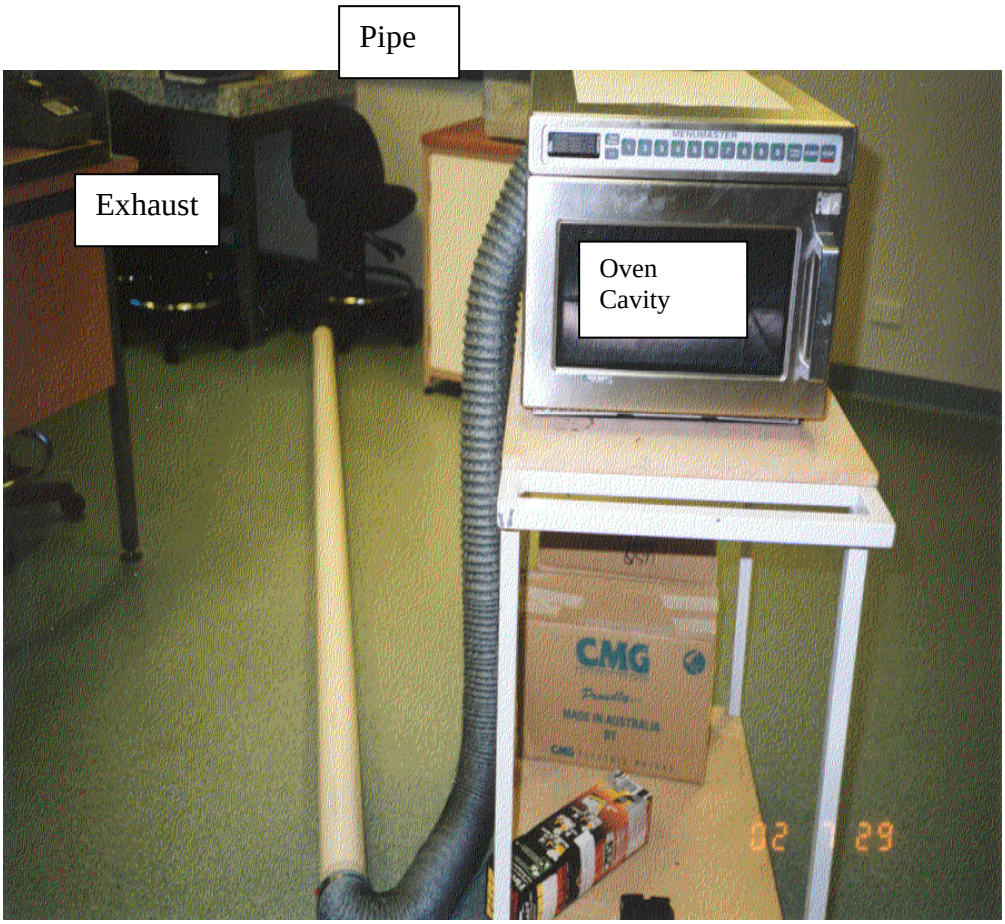

Figure 6.6: The modified oven and its peripherals (Ku, H S 2002b).

6.4.2 Type of the Microwave Exposure Time

There are six types of conditions for the microwave exposure of the specimen. They are 540-Watt power with exposure of 15 seconds, 20 seconds and 25 seconds, and 720-Watt power with exposure of 15 seconds, 20 seconds and 25 seconds.

Below is the table 6.2 show the changes in volume and other parameters of vinyl ester composites during exposed to the different power levels and exposure times. The shrinkage problem did not exist in the short specimen as there were some slots in the specimen and the specimen size was small.

Table 6.2: Volume shrinkage and other parameters for 400 ml of VE/FLYASH (33%) exposed to 180-W microwaves at different duration.

Microwave exposure time (seconds)	0	55	60	65
Oven cavity Temperature (^{o}C)	16	24	22	22
Relative humidity (%)	52	48	46	47
Temperature after microwave exposure	NA	30	32	34
Original volume (ml)	400	400	400	400
Final volume (ml)	363.64	387.69	389.26	390.81
Volume shrinkage (%)	9.09	3.00	2.70	2.30
Volume at maximum temperature (ml)	382.2	392.2	393.9	394.1
Time to reach gel time (minutes)	62.5	7.0	7.0	6.0
Maximum temperature	139	138	148	150
Time to reach maximum temperature (minutes)	67.5	10.0	10.0	9.0

Chapter 7. Test Rig and Apparatus

7.1 Test Rig Requirements

The test rig configuration for the MTS 810 Material Testing Systems was modified. So that we can obtain the accurate results, the requirements as shown as the follow:

- The loading mechanism can provide adequate tensile force.
- The grippers used will not deform during testing.
- The alignment of the grippers is accurate.
- The grippers are allowed for adequate control of the load line position.
- The plastic deformation of the specimen apex caused by the grippers should be minimized.

7.2 Test Rig Available

There are several test rig purposely designed for the short rod or bar test method. Some of the test rigs are incorporated with other advanced computer systems like fractometer in order to produce the result more accurately and consistently. However, the test rig should be chosen according to its availability, functionality and suitability.

7.3 MTS 810 Material Testing Systems

In this study, for the short bar tensile testing, The MTS 810 material testing systems (figure 7.1) was used, it especially for small size specimen. The fracture toughness of the short bar specimen was tested by an opening tensile load applied at the opening of the specimen by grippers as shown in figure 7.2. Finally the detailed information results will print out by MTS 810 material testing systems. It attached in appendix D.

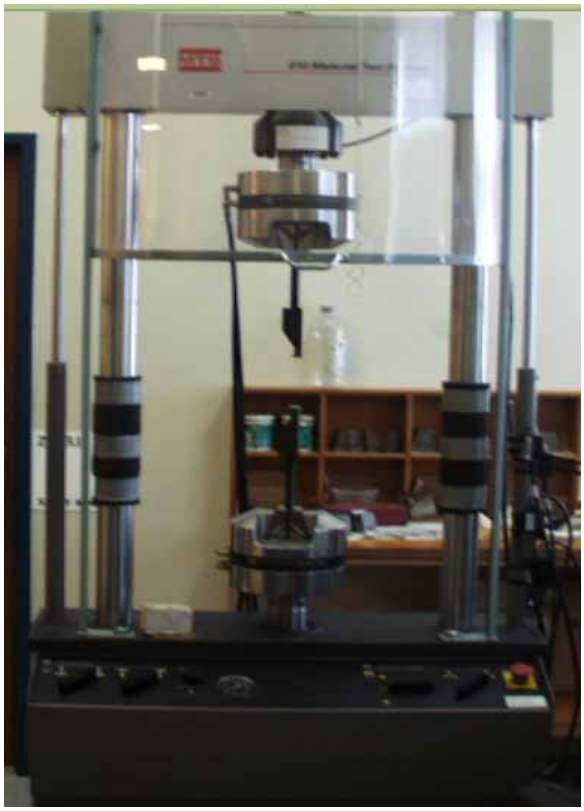

Figure 7.1: MTS 810 Material Testing Systems.

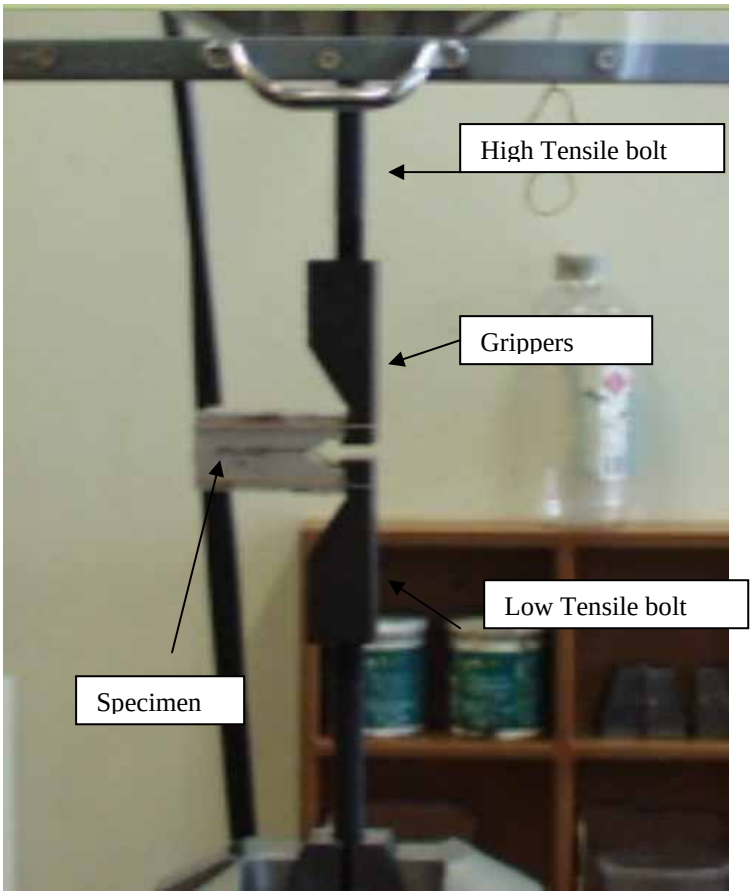

Figure 7.2: Test rig with specimen in position.

7.4 The Advantages of MTS 810 Material Testing Systems

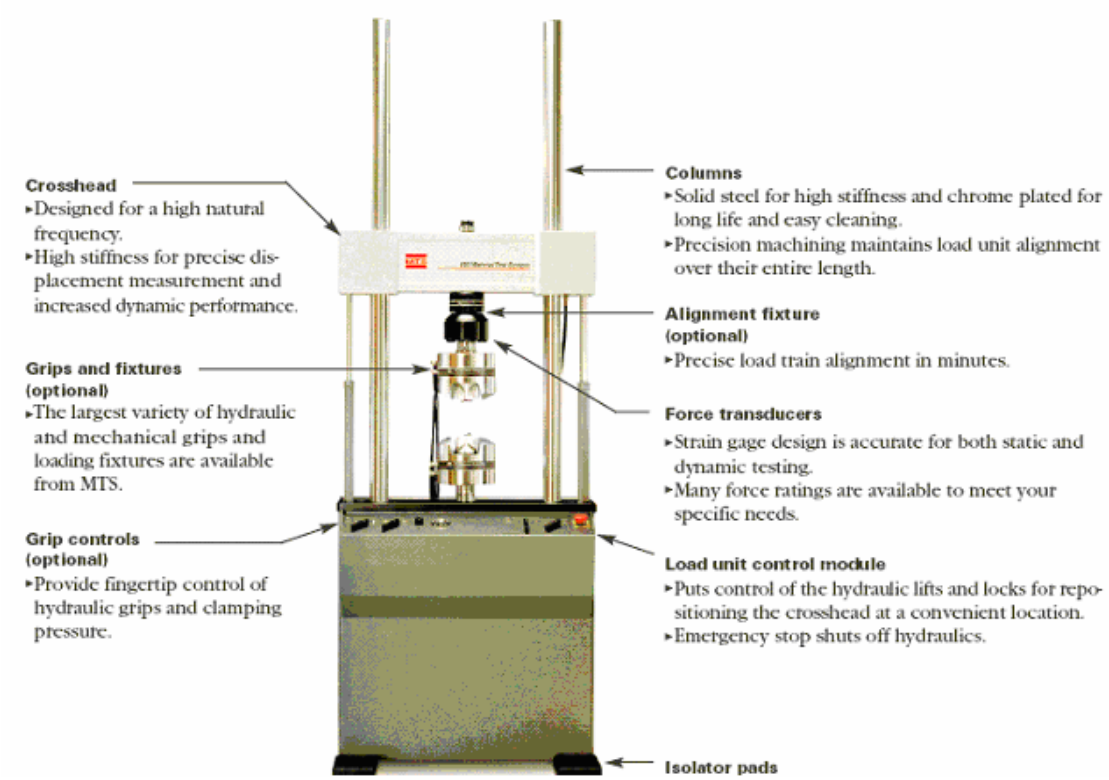

Figure 7.3: The systems of MTS 810 Material Testing Systems (MTS 810 FlexTest™ Material Testing Systems).

The MTS 810 machine was used because its advantages over then other test rig, its advantages are as following:

- **Flexibility:** It can be used for many types of testing such tensile testing, fatigue life studies, Asphalt or soil testing and etc by simply changing or adjusting its grips and fixtures.

- **User-friendly:** The testing systems are incorporated with the TestStart IIs control system, which is consisted of three major parts: the TestStar system software, the digital controller, and a remote station control panel as shown in

figure 7.5.The control system is able to produce the result in the form of graph or table with the ready programmed software. Meanwhile some of the important statistical variable such as mean and standard deviations are included in result as well.

- **Accuracy:** Its superior axial and lateral stiffness are achieved through an integral actuator design, stiff, but low mass crosshead, and specially force transducer.

7.5 Gripper Design

In this project, the MTS 810 Material Testing System was used. It was because MTS 810 machine is more suitable for tensile testing involving smaller load and can provides more accurate results. Slight modification was made to the grippers to enable them to be placed to the machine. The grippers were hold by high tensile bolts as shown in figure 7.2. There are four alternatives to design the grippers as illustrated in the figure 7.4.

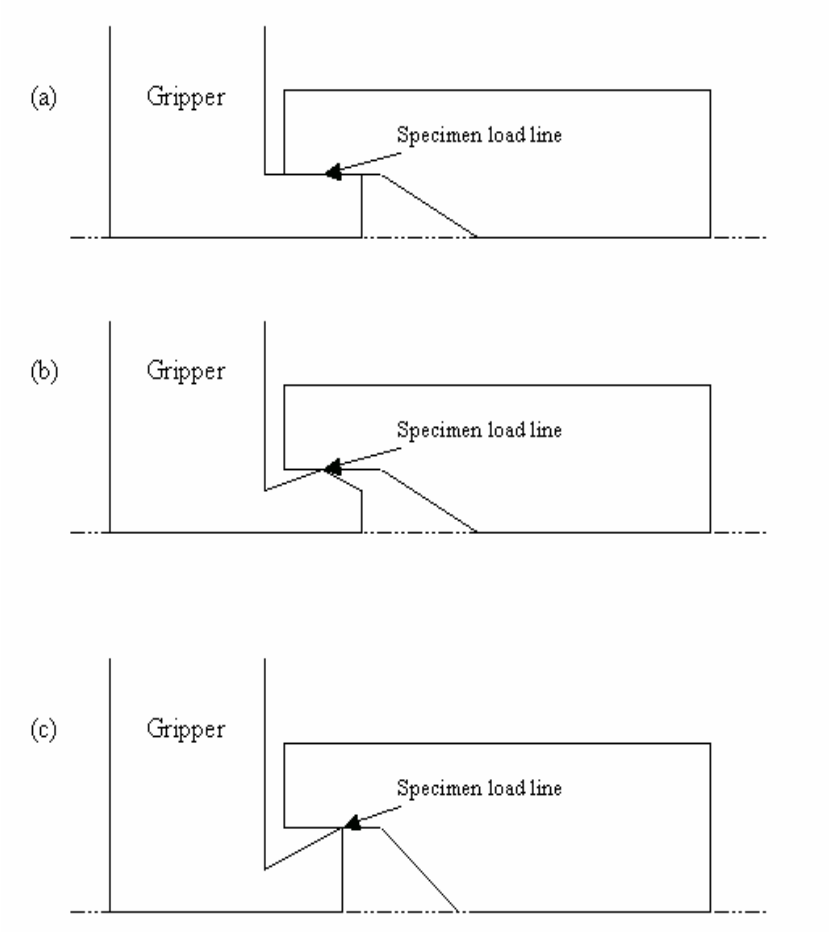

Figure 7.4 Grippers designs.

The gripper shown in figure 7.4(c) was chosen because the load line positioning was good and it was easier to manufacture. However, the stress concentration occurred in the sharp corner so the grippers failed before the load reached 25 KN and the opening of the specimen was opened. After some modification, Phelan (1990) designed rounded profile grippers, while the profile from previous sample was ground out as illustrated in figure 7.5.

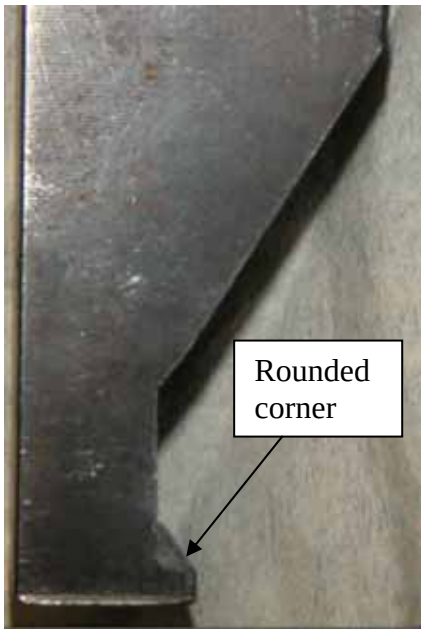

Figure 7.5: The rounded profile of the grippers.

7.5 Scanning Electron Microscopy (SEM)

Scanning electron microscopy as shown in figure 7.6 is commonly used for surface morphology analysis. In order to view non-conductive samples such as ceramics or plastics, we must cover the sample with a thin layer of a conductive material. We do this using a small device called a sputter coater.

Figure 7.6: The system of the Scanning Electron Microscopy (SEM)

7.5.1 Specimen Preparation for SEM

The purpose of the sputter coater as shown in figure 7.7 is to make non-metallic samples electrically conductive. Uses argon gas and a small electric field. The sample is placed in a small chamber that is at vacuum. Argon gas is then introduced and an electric field is used to cause an electron to be removed from the argon atoms to make the atoms ions with a positive charge. The Ar ions are then attracted to a negatively charged piece of gold foil. The Ar ions act like sand in a sandblaster, knocking gold atoms from the surface of the foil. These gold atoms now settle onto the surface of the sample, producing a gold coating.

Figure 7.7: A sputter coater coats the sample with gold atoms (Lowa State Unversity Material Science & Engineering DEPT.)

The vinyl ester composite samples are non-conductive so they had to be made conductive by coating them with a conductive coat. The conductive coat can be either gold or carbon; both are applied in an evaporation unit. The carbon coating is used when the sample will be analysed using X-rays. The carbon acts as an invisible coating to the X-rays. The gold coating is used for imaging when composition data of the sample is not required. The gold coating is a finer layer than the carbon coating. Therefore better resolution of the surface can be achieved.

Chapter 8. Latin Square

8.1 Introduction of Latin Square

A Latin square is used in experimental designs in which one wishes to compare treatments and to control for two other known sources of variation. To use a Latin square for an experiment comparing n treatments we will need to have n levels for each of the two sources of variation for which we wish to control. Latin squares were first used in agricultural experiments. It was recognized that within a field there would be fertility trends running both across the field and up and down the field. So in an experiment to test, say, six different fertilisers, A, B, C, D, E and 1, the field would divided into six horizontal strips and six vertical strips, thus producing 36 smaller plots. A Latin square design will give a random allocation of fertiliser type to a plot in such a way that each fertiliser type is used once in each horizontal strip (row) and once in each vertical strip (column). Such a layout is shown in Fig. 8.1.

1	A	B	C	D	E
B	1	A	D	E	C
A	B	1	E	C	D
C	D	E	1	A	B
D	E	C	B	1	A
E	C	D	A	B	1

Figure 8.1: A Latin square design for six treatments.

The most important application of the Latin Square is the design of statistical experiments. Let us say that we are interested in finding fracture toughness of particulate reinforced vinyl ester composite by curing them under microwave exposure, and would like to have the least effect (the value of fracture toughness which is closest to ambient condition) possible. The variables here are the exposure duration and power levels and assume that the volume of the composite used is constant, say 100 millilitres. These are called treatments. We want to know what treatments are the most acceptable for reducing shrinkage of the composite, and by how much, and which are worthless, so we can weight the economic alternatives.

Latin Square is a multiplication table in the form of a matrix. An example of it is given in Table 8.1. This is a multiplication table for any group whose six different fertilisers correspond to A, B, C, D, E and 1. They can be numbers. A group is a set of elements that is closed under whatever "multiplication" is defined for them. This means that the result of any multiplication is again a member of the group. Furthermore, the group must contain the identity element (corresponding to 1) and the inverse A to any element B, such that AB = BA = 1. A is usually written V^{-1}. The multiplication must also be associative, i.e. (AB) C = A (BC) for any three members A,B,C of the group. The requirements for the identity and the inverse mean that no element is repeated in any row or column, so that each row or column contains each element once and once only. This is the strict definition of a Latin Square (Denes and Keedwell, 1974).

8.2 Advantage & Disadvantage of Latin Square

The advantages of Latin square designs are:

1. They handle the case when we have several nuisance factors and we either cannot combine them into a single factor or we wish to keep them separate.
2. They allow experiments with a relatively small number of runs.

The disadvantages are:

1. The number of levels of each blocking variable must equal the number of levels of the treatment factor.
2. The Latin square model assumes that there are no interactions between the blocking variables or between the treatment variable and the blocking variable.

8.3 Methodology of Latin Square

During the experiments, we collected the shrinkage results from *n* experiments, so we can find an average fracture toughness $X = \frac{\sum x}{n}$, where x is the fracture toughness from one of the *n* experiments. On the other hand, the quantity $v = \Sigma(x-X)^2$ is always positive, and gives an indication of the individual values differ from the mean. It is identified the variance. If the variation is due to random causes, it is quite possible that the different fracture toughness values are statistically distributed according to the normal distribution, the bell-shaped curve that is so familiar. If so, then the average of the normal distribution is around X, and its standard deviation σ around $\sigma^2 = \frac{v}{N-1}$.

The accuracy of these estimates increases as *n* increases. *n*-1 is called the number of degrees of freedom associated with the variance.

At present suppose we have six treatments. In order to distribute the treatments somewhat evenly over the test plot, we do not need a group of multiplication table; any of the many Latin Square can be used. We now cure the composite under microwave conditions, and associate a fracture toughness x with each of the 36 plots. The total variance *v* is partly due to the random effects on shrinkage that would occur with any treatment, and the differences due to treatments. It is possible to separate the total variance *v* into components due to rows, columns, treatments, and "errors". This is called Analysis of Variance, AOV. The variance due to rows is n (here n = 6) times the sum of the squares of the deviations of the row averages from the grand average, and similarly for the column and treatment averages. The total variance, less these three partial variances, gives the residual, or error, variance.

If the error were the only reason for the differences in fracture toughness, the fracture toughness could be assumed that it was distributed accordingly to the same normal distribution, with the same standard deviation. Then, all the estimates of the standard deviation would be about the same, whether from the row, column, treatment, or error variances. The row, column and treatment variances have n-1 (here, 5) degrees of freedom and the error has (n-1) (n-2) degrees of freedom (here, 20). The sum of all these degrees of freedom is *n*-1 (here, 35), the number of degrees of freedom of the overall variance. If we now divide each variance by its degrees of freedom we get the estimates of the population variance σ^2.

These estimates will not all be the same. Not only are they just estimates with statistical error, the treatments for example, might actually be effective. Whether the differences in the estimates are simply due to chance can be investigated by dividing

the row, column and treatment estimates by the error estimate. Finally, we can list out a table as shown in table 8.1.

Table 8.1: Results of statistical calculations (http://www.tfrec.wsu.edu/ANOVA/Latin.html)

Source of variation	Degrees of freedom[a]	Sums of squares (SSQ)	Mean square (MS)	F
Rows (*R*)	r-1	SSQ_R	$SSQ_R/(r-1)$	MS_R/MS_E
Columns (*C*)	r-1	SSQ_C	$SSQ_C/(r-1)$	MS_C/MS_E
Treatments (*Tr*)	r-1	SSQ_{Tr}	$SSQ_{Tr}/(r-1)$	MS_{Tr}/MS_E
Error (*E*)	(r-1)(r-2)	SSQ_E	$SSQ_E/((r-1)(r-2))$	
Total (*Tot*)	r^2-1	SSQ_{Tot}		
[a]where r=number of treatments, rows, and columns.				

This statistic is called F, and there are tables showing how large F can be just due to chance. One usually takes a value that is exceeded by chance only 1% of the time as the criterion of significance. If the treatments really do have an effect, it will probably show up quite distinctly in the F values (University of Denver, 2003, pp. 1-3). The significant values of F depend on the degrees of freedom of the two estimates used, here 5 and 20 (as shown in Table 8.2) (Murdoch, and Barnes, 1952). Statistical table (see bold portion in Table 8.2) gives the 1% value of F as 4.10 in this case. The 5% value is only 2.71 (see bold portion in Table 8.2). If the ratio of the estimates is larger than 4.10 for the treatments, we can be fairly sure that they have a real effect on the fracture toughness of composites. Then we can enquire further into how the fracture

toughness is affected by the treatments with some appreciation of the reliability of our conclusions.

Table 8.2: (Part of) Percentage Points of the F Distribution.

v_1 / v_2	**1**	**2**	**3**	**4** ↓	**5**
14	4,60 (6.30) 8.86 17.14	3.74 (4.86) 6.51 11.78	3.34 (4.24) 5.56 9.73	3.11 (3.89) 5.04 8.62	2.96 (3.66) 4.70 7.92
16	4.41 (6.12) 8.53 16.12	3.63 (4.69) 6.23 10.97	3.24 (4.08) 5.29 9.01	3.01 (3.73) 4.77 7.94	2.85 (3.50) 4.44 7.27
18	4.41 (5.98) 8.29 15.38	3.55 (4.56) 6.01 10.39	3.16 (3.95) 5.09 8.49	2.93 (3.61) 4.58 7.46	2.77 (3.38) 4.25 6.81
→ 20	4.35 (5.87) 8.10 14.82	3.49 (4.46) 5.85 9.95	3.10 (3.86) 4.94 8.10	2.87 (3.51) 4.43 7.10	**2.71** **(3.29)** **4.10** **6.46**

8.4 An example of Latin Square

Table 8.3 is a table of fracture toughness values found in tests.

Table 8.3 Table of Latin squares for fracture toughness.

x (50.85)	y (48.81)	z (48.96)	u (47.52)	v (51.04)
y (51.84)	z (48.62)	u (48.09)	v (48.20)	x (54.10)
z (48.39)	u (48.55)	v (50.74)	x (50.85)	y (51.72)
u (53.91)	v (52.97)	x (50.85)	y (49.47)	z (48.49)
v (51.88)	x (49.47)	y (48.47)	z (51.04)	u (46.99)

Table 8.4 is a table showing the sum, the average of each row respectively. It also shows the deviation ^{2*} of each row. With reference to Table 8.4, a calculation for row is illustrated as follows:

Table 8.4: Table of rows' calculations.

Number of row	Sum of Row	Average	Deviation ^{2}
1	247.18	49.44	0.37
2	250.85	50.17	0
3	250.32	50.06	0
4	255.69	51.14	1.12
5	247.85	49.57	0.26
		$\overline{\overline{X}} = 50.08$	$\sum \text{Dev}^2 = 1.75$

- $^{*}Deviation^2\ for\ Row1, = (\text{row1}_{\text{average}} - \overline{\overline{X}})^2 = (49.44 - 50.08)^2 = 0.37$

  where $\overline{\overline{X}}$ is the grand average

- *Sum of Square for row* = $\sum \text{Dev}^2 \times \text{n} = 1.75 \text{ x } 5 = 8.75$, which is then placed in the sum of square for row in Table 8.8.

- The degree of freedom, *DF*, for row is (n – 1) = 5 – 1 = 4, which is put into the *DF* of row of Table 8.8.

Table 8.5 is a table showing the sum, the average of each column respectively. It also shows the deviation ^{2*} of each column.

Table 8.5: Table of columns' calculations.

Number of column	1	2	3	4	5	
Sum of column	256.87	248.42	247.11	247.08	252.34	
Average	51.37	49.69	49.42	49.42	50.47	
Deviation^2	1.66	0.15	0.44	0.44	0.15	$\sum$ Dev^2 = 2.84

- *Sum of Square for column* = $\sum$ Dev$^2\times$ n = 2.84 x 5 = 14.20, which is similarly placed in the sum of square for column in Table 8.8.

- The degree of freedom, *DF*, of column is (n – 1) = 5 – 1 = 4, which is put into the DF of column of Table 8.8.

Table 8.6 is a table showing the sum, the average of each treatment respectively. It also shows the deviation ^{2*} of each treatment.

Table 8.6: Table of treatments' calculations.

Treatment type	X	Y	Z	U	V	
Treatment Average	51.22	50.06	49.10	49.01	50.97	
Treatment Deviation ^{2}	1.30	0	0.96	1.15	0.79	$\sum$ Dev^2 = 4.20

- *The treatment average for U* = $\frac{47.52 + 48.09 + 48.55 + 53.91 + 46.99}{5} = 49.01$

- *The treatment deviation ^{2} for U* = $(49.01 - \overline{\overline{X}})^2 = (49.01 - 50.08)^2 = 1.15$

- *Sum of Square for treatment* = $\sum$ Dev$^2\times$ n = 4.20 x 5 = 21.00, which is similarly placed in the sum of square for treatment in Table 8.8.

- The degree of freedom, *DF*, of treatment is (n – 1) = 5 – 1 = 4, which is put into the DF of treatment of Table 8.8.

Table 8.7 is a table showing deviation ^{2} of each individual entry in Table 8.3.

Table 8.7: Calculations of total value.

0.59	1.61	1.26	6.55	0.92
3.10	2.13	3.96	3.54	16.16
2.86	2.34	0.44	0.59	2.69
14.67	8.35	0.59	0.37	2.53
3.24	0.37	2.59	0.92	9.55

$(X_{5,1} - \overline{\overline{X}})^2 = (51.88 - 50.08)^2 = 3.24.$

- The entries above are obtained as shown in the above example.
- *Sum of Square for total* = $\sum$ Dev^2 = 91.92, which is similarly placed in the sum of square for treatment in Table 8.8.
- The degree of freedom, *DF*, for total = ($n^2 - 1$) = 25 – 1 = 24, which is put into the *DF* of treatment of Table 8.8.
- *Degree of freedom for error* = 24 – 4 – 4 -4 = 12
- *Sum of square of error* = 91.92 – 8.75 – 13.45 – 21.00 = 48.72, which is then inserted into Table 8.8.

The values obtained from above are filled in the table below for the statistical calculations. While the percentage point of F distribution can be found from table of Latin square in appendix E.The result obtained will be further discussed in chapter 9.

Table 8.8: Results of statistical calculations.

Source	**D.F.**	**Sum Sq.**[##]	**Estimate**[#]	**F**[!]
Rows	4	8.75	2.19	0.55
Columns	4	14.20	3.55	0.84
Treatments	4	21.00	5.25	1.31
Error	12	48.72	4.00	-------
Total	24	91.92	---------	-------

$$^{\#}\text{Estimate for row} = \frac{Sum \quad of \quad Square}{DF} \qquad \text{(Eqn 8.1)}$$

$$= \frac{8.75}{4} = 2.19$$

$$\text{\# Estimate for error} = \frac{Sum \quad of \quad Square}{DF} \qquad \text{(Eqn 8.2)}$$

$$= \frac{48.72}{12} = 4.00$$

$$\text{! F for row} = \frac{Estimate}{Error} \qquad \text{(Eqn 8.3)}$$

$$= \frac{2.19}{4} = 0.55$$

$$\text{! F for treatment} = \frac{Estimate}{Error} \qquad \text{(Eqn 8.4)}$$

$$= \frac{5.25}{4} = 1.31$$

Chapter 9. Results and Discussions

9.1 Introduction

This chapter presents the results obtained from the experimental work. The chapter will be divided into sections; one is related to e tensile testing results from the experimental work, the other is fracture toughness determination and discussions. After this Latin Square for the fracture toughness will be analyzed; the next thing is comparisons of results of the fracture toughness and other parameters for VE cured under different conditions. In last section, the specimens cured in ambient conditions will be compared with those cured with microwave conditions having power levels of 180 Watts, 360 Watts, 540 Watts and 720 Watts respectively. The last section will be fractured surface analysis using SEM, in which five critical points of the fractured surface to be analyzed. At the end of this chapter, comparison on 540 Watts microwave power with 25 seconds specimen and 720 Watts microwave power with 20 seconds specimen will be made.

9.2 MTS-810 tensile testing machine

This is the test used to calculate the fracture toughness. During the test, a constantly increasing force will apply at the top edge of the specimen until the load reaches a maximum and crack occurred. A crack forms at the tip of the notch would proceed down the specimen along the notched path. By knowing the location of the crack at the maximum load under linear elastic fracture condition and the height of the crack that

corresponds to the maximum constant load force, the fracture toughness of the composite can be calculated. Specimens for test were shown in Figure 9.1.

Figure 9.1: The fractured specimens and show the part for making the chevron slot

The curing conditions in this project were divided into three major groups. First condition is cured under ambient conditions; second condition is cured under 540 Watts microwave conditions and third condition is cured under 720 Watts microwave conditions. With a power of 540 Watts, exposure times were 15 seconds, 20 seconds and 25 seconds; with a power of 720 Watts exposure times were 15 seconds, 20 seconds and 25 seconds. The raw data for all curing conditions are shown in Appendix C. The tensile testing results generated by MTS-810 machine included the peak load, failure load, break load, peak load elongation and the break load elongation of the specimen. Figure 9.2 showed the generated graph from a tensile testing.

The three phases listed decide weather the specimen tensile testing has been successful or not.

- First phase – The tensile testing started with the speed of 1mm/min, which results in the increased load to initiate the specimen crack
- Second phase – When the specimen passes its peak load, the specimen will show elongation behaviour.
- Third phase - The crack will be elongated and will reach point 4 of the five critical points shown in Figure 9.3 and the specimen will show brittle behaviour in this area.

It some of the samples, for example the 720 Watts power level with 20 seconds of exposure time (Figure 9.4), a small amount of energy cracked the sample but the real situation is that high energy was required because a loud cracking sound was made when it cracked. This happen, due to the cause of a bad quality mould. Barker (1980) defined this effect as crack curve jumping as illustrated in Figure 9.4. Therefore this specimen is not fully fractured but accruing the crack at the side of it.

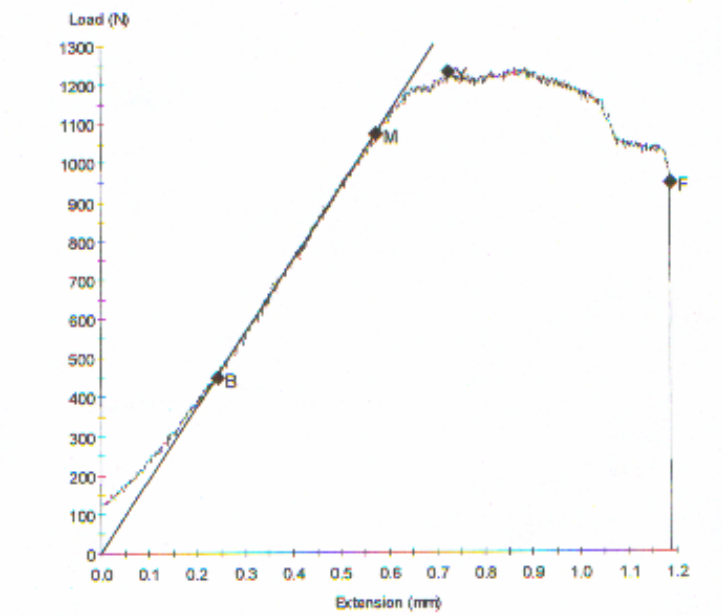

Specimen Results:

Name	Value	Units
Width	20.000	mm
Area	1000	mm^2
Peak Load	1238	N
Peak Stress	1.24	MPa
Elongation at Peak	0.884	mm
Break Load	942	N
Break Stress	0.94	MPa
Elongation At Break	1.188	mm
Stress At Offset Yield	1.207	MPa
Load At Offset Yield	1206.898	N

Figure 9.2: The change of load versus crack length of a sample cured under microwave condition (540 Watt power level and 15-second exposure time).

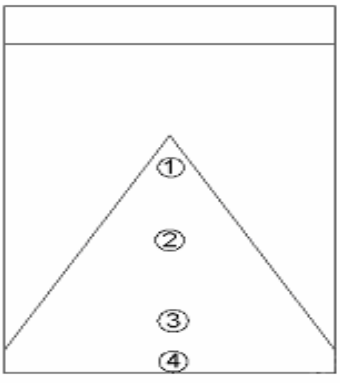

Figure 9.3: Five critical points for the fractures surface to be analyzed.

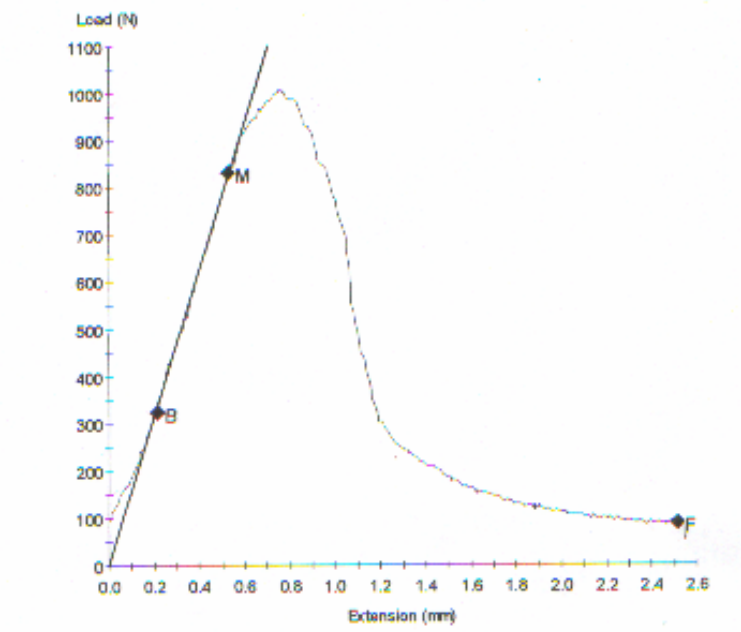

Specimen Results:

Name	Value	Units
Width	20.000	mm
Area	1000	mm^2
Peak Load	1008	N
Peak Stress	1.01	MPa
Elongation at Peak	0.752	mm
Break Load	88	N
Break Stress	0.09	MPa
Elongation At Break	2.515	mm
Stress At Offset Yield	1.004	MPa
Load At Offset Yield	1003.754	N

Figure 9.4: The change of load versus crack length of a sample cured under microwave condition (720 Watt power level and 15-second exposure time).

9.3 Fracture Toughness Determinations and Discussion

The purpose of the fracture toughness is to determine the severity of a pre-existing defect in term of its tendency to initiate a fracture. The critical fracture toughness value K_{IC} was determined with the compact specimens using 5 % secant method. To determine the

fracture toughness (K_{IC}) of a material with the standard test methods, the K-calibration was made according to the ASTM E399-78.

For the evaluation of K-calibration, K was calculated from the maximum load applied from the tensile testing and the crack length (Figure 9.5).

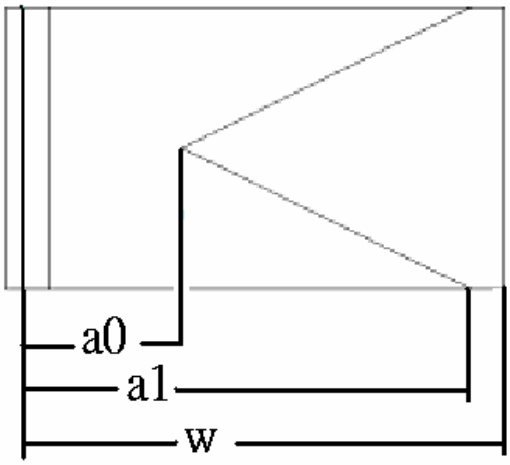

Figure 9.5: Cross-section dimension of short bar specimen.

9.3.1 The formulas and methods for calculating the fracture toughness

The specimen cured with a microwave power of 540 watt with 25 seconds exposure time was taken as an example. The formulas and methods to obtain the fracture toughness were illustrated as follows:

The formulas used to calculate the fracture toughness were Equations 9.1 through 9.4.

$$K_{ICSB} = \frac{(F_{max} Y_m^*)}{B\sqrt{W}} \qquad \text{(Eqn. 9.1)}$$

where F_{max} = Peak load

Y_m^* is the compliance calibration according to ASTM E-399-78 standard.

$$\omega = \frac{W}{H} = \frac{73.7}{44.2} = 1.667 \qquad \text{(Eqn. 9.2)}$$

$$\alpha_0 = \frac{a_0}{W} = \frac{24.4}{73.7} = 0.331 \qquad \text{(Eqn. 9.3)}$$

$$\alpha_1 = \frac{a_1}{W} = \frac{63.8}{73.7} = 0.866 \qquad \text{(Eqn. 9.4)}$$

The calculations for it were made by Munz (1981).

$$Y_m^* = \{- 0.36 + 5.48\omega + 0.08\omega^2 + (30.65 - 27.49\omega + 7.46\omega)\,\alpha_0 + (65.90 + 18.44\omega - 9.76\omega)\alpha_0^2\} \left\{\frac{\alpha_1 - \alpha_0}{1 - \alpha_0}\right\}^{\frac{1}{2}}$$

$Y_m^* = 16.5013$

The results of the 540-Watt power level and 25-second cured group (six specimens) were shown in Table 9.1. The mean ($\bar{\mu}$) of fracture toughness is 46.73 N.mm $^{-3/2}$.

Table 9.1: Test results of 540 Watts and 25-second exposure.

Specimens	***Elongation at Peak (mm)***	***Peak load (N)***	***Elongation at Break (Mm)***	***Break Load (N)***	***Fracture Toughness (N.mm $^{-3/2}$)***
Table 9.1: Test results of 540-Watt power and 25-second.					
1	1.260	1214	1.626	921	45.93
2	0.920	1260	1.292	862	47.67
3	1.227	1304	1.629	817	49.34
4	1.180	1176	2.087	777	44.50
5	1.208	1230	1.526	809	46.54
6	1.22	1226	1.391	812	46.39
Mean	1.23	1235	1.592	833	46.73
Standard Deviation	0.04	43	0.276	51	1.64

Using $$K_{ICSB} = \frac{(F_{max} Y_m^{*})}{B\sqrt{W}}$$ (Eqn. 9.5)

and let B = 50.8 (by design),

$$W = 73.3 ,$$

From the Table 9.1 mean of Peak Load = F_{max} = 1235 N

and Y_m =16.5013

therefore $K_{ICSB} = \frac{(1235x16.5013)}{50.8\sqrt{73.3}} = 46.73$ (N.mm $^{-3/2}$)

9.3.2 Results of all other groups of Specimens:

For this experiment, we divided into six group, those were 540 Watts and 15 second, 20 second and 25 second exposure time and 720Watts and 15 second, 20 second and 25 second exposure time, and each group have six specimens. For the mean fracture toughness, we will take the average of all six specimens in the same group. So we can observe that the mean of fracture toughness is become around 35 N.mm $^{-3/2}$ to 48 N.mm $^{-3/2}$. The results as shown as below table 9.4 – table 9.6

1. Test results of 540 Watts and 15seconds

Table 9.2: Test results of 540 Watt s and 15 seconds.

Specimens	***Elongation at Peak (mm)***	***Peak load (N)***	***Elongation at Break (Mm)***	***Break Load (N)***	***Fracture Toughness (N.mm $^{-3/2}$)***
1	1.228	1179	1.541	883	44.73
2	0.973	1248	1.223	870	47.35
3	1.611	1479	1.698	1332	56.11
4	0.728	1230	1.172	1024	46.67
5	0.795	1232	0.970	1062	46.74
Mean	1.07	1273.6	1.32	1034.2	48.32
Standard Deviation	0.36	117.71	0.29	186.67	4.46

2. Test results of 540 Watts and 15seconds

Table 9.3: Test results of 540 Watts and 20 seconds.

Specimens	***Elongation at Peak (mm)***	***Peak load (N)***	***Elongation at Break (Mm)***	***Break Load (N)***	***Fracture Toughness ($N.mm^{-3/2}$)***
1	0.781	1013	1.183	649	38.43
2	0.810	1169	1.321	842	44.35
3	0.723	920	1.019	626	34.91
4	1.525	1198	1.602	1045	45.45
5	0.791	679	1.147	345	25.76
Mean	0.93	995.8	1.25	701.4	37.78
Standard Deviation	0.34	210.53	0.22	261.38	7.99

3. Test results of 720 Watts and 15 seconds

Table 9.4: Test results of 720 Watts and 15 seconds.

Specimens	***Elongation at Peak (mm)***	***Peak load (N)***	***Elongation at Break (Mm)***	***Break Load (N)***	***Fracture Toughness ($N.mm^{-3/2}$)***
1	1.325	1282	1.637	1116	48.64
2	1.214	1162	1.461	1098	44.09
3	0.752	1008	2.515	88	38.24
4	1.345	1191	1.711	1091	45.19
5	1.098	1176	1.835	266	44.62
6	1.661	1067	1.674	1066	40.48
Mean	1.232	1148	1.806	788	43.56
Standard Deviation	0.301	97	0.368	476	3.36

4. Test results of 720 Watts and 20 seconds

Table 9.5: Test results of 720 Watts and 20 seconds.

Specimens	***Elongation at Peak (mm)***	***Peak load (N)***	***Elongation at Break (Mm)***	***Break Load (N)***	***Fracture Toughness ($N.mm^{-3/2}$)***
1	1.079	1055	1.346	911	40.03
2	0.971	1027	1.189	700	38.96
3	0.704	921	0.979	443	34.94
4	1.659	1310	1.659	1310	49.70
5	1.126	1222	1.126	1222	46.36
6	0.722	962	0.934	811	36.50
Mean	1.043	1083	1.206	900	41.08
Standard Deviation	0.350	152	0.267	325	5.77

5. Test results of 720-Watt power and 25-second

Table 9.6: Test results of 720 Watts and 25 seconds.

Specimens	***Elongation at Peak (mm)***	***Peak load (N)***	***Elongation at Break (Mm)***	***Break Load (N)***	***Fracture Toughness ($N.mm^{-3/2}$)***
1	1.116	1219	1.499	1004	46.25
2	0.922	1208	1.342	725	45.83
3	1.524	1279	1.784	1019	48.53
4	0.958	1110	1.378	777	42.11
5	1.314	1243	1.778	901	47.16
Mean	1.167	1212	1.556	885	45.98
Standard Deviation	0.253	63	0.213	132	2.40

9.4 Latin Square Analysis

Consider Latin Square (Denes and Keedwell, 1974; University of Denver, 2003) and assign the following symbols for the different treatments of the VE/FLYASH (33%). The six treatments are U, V, W, X and Y and a 5 x 5 Latin Square are used. Fracture toughness of composites are as follows (Table 9.7):

where

U: 540W (15s), V: 540 W (25s), W: 720 W (15s),
X: 720 W (25s) and Y: Ambient cured.

Table 9.7: Latin square for fracture toughness.

U 44.73	V 45.93	W 48.64	X 46.25	Y 51.04
V 47.67	W 44.09	X 45.83	Y 48.20	U 47.35
W 38.24	X 48.53	Y 50.74	U 56.11	V 49.34
X 42.11	Y 52.97	U 46.47	V 44.50	W 48.19
Y 51.88	U 46.74	V 46.54	W 44.62	X 47.16

For the table 9.8 is a table showing the sum, the average of each row respectively. It also shows the deviation ^{2*} of each row.

Table 9.8: Calculations for rows.

Number of row	Sum of Row	Average	Deviation ^{2}
1	236.59	47.32	0.0016
2	233.14	46.63	0.533
3	242.96	48.59	1.51
4	234.24	46.85	0.26
5	236.94	47.39	0.0009
		$\overline{\overline{X}}$ = 47.36	$\sum$ Dev^2 = 2.31

Table 9.9 is a table showing the sum, the average of each column respectively. It also shows the deviation ^{2*} of each column.

Table 9.9: Calculations for Columns.

Number of column	1	2	3	4	5	
Sum of column	224.63	238.26	238.22	239.68	243.08	
Average	44.93	47.65	47.64	47.97	48.62	$\overline{\overline{X}} = 47.36$
Deviation^2	5.91	0.0841	0.0784	0.372	1.59	$\sum \text{Dev}^2 = 8.034$

Table 9.10 is a table showing the sum, the average of each treatment respectively. It also shows the deviation ^{2*} of each treatment.

Table 9.10: Calculations for treatments

Treatment type	U	V	W	X	Y	
Treatment Average	48.28	46.8	44.76	45.98	50.97	$\overline{\overline{X}} = 47.36$
Treatment Deviation ^{2}	0.85	0.31	6.76	1.904	13.03	$\sum \text{Dev}^2 = 22.854$

Table 9.11 is a table showing deviation ^{2} of each individual entry in Table 9.7.

Table 9.11: Calculations for total values.

6.92	2.04	1.64	1.23	13.54
0.096	10.70	2.34	0.71	0.0001
83.17	1.37	11.42	76.56	3.92
27.56	31.47	0.792	8.18	0.69
20.43	0.38	0.67	7.51	0.04

Table 9.12 is a table that to calculate the total of sum of square for the Results of statistical calculations as shown as in table 9.13.

Table 9.12: Sum of Square for total = $\sum$ Dev^2 = 313.3781

6.92	2.04	1.64	1.23	13.54	25.37
0.096	10.7	2.34	0.71	0.0001	13.8461
83.17	1.37	11.42	76.56	3.92	176.44
27.56	31.47	0.792	8.18	0.69	68.692
20.43	0.38	0.67	7.51	0.04	29.03
					313.3781

If all variables are taken into account when establishing the Latin Square, the matrix will be a 5 x 5 matrix (Table 9.7). Details of the calculations as shown in the chapter 8 and the results are shown in Table 9.13.

Table 9.13: Results of statistical calculations.

Source	D. F.	Sum Sq.##	Estimate#	F !
Rows	4	11.55	2.89	0.24
Columns	4	40.17	10.04	0.82
Treatments	4	114.27	28.57	2.33
Error	12	147.39	12.28	-------
Total	24	313.38	-------	-------

$$^{\#}\text{Estimate for row} = \frac{Sum \quad of \quad Square}{DF} \qquad \text{(Eqn. 9.6)}$$

$$= \frac{11.55}{4} = 2.89$$

$$^{\#}\text{Estimate for error} = \frac{Sum \quad of \quad Square}{DF}$$

$$= \frac{147.39}{12} = 12.28 \qquad \text{(Eqn. 9.7)}$$

$$\text{F for row} = \frac{Estimate}{Error} \qquad \text{(Eqn. 9.8)}$$

$$= \frac{2.89}{12.28} = 0.24$$

Table 9.14: (Part of) Percentage points of the F distribution.

v_1 / v_2	**1**	**2**	**3**	**4**	**5**
9	5.12 (7.21) 10.56 22.85	4.26 (5.71) 8.02 16.39	3.86 (5.08) 6.99 13.90	3.63 (4.72) 6.42 12.56	3.48 (4.48) 6.06 11.71
10	4.96 (6.94) 10.04 21.04	4.10 (5.46) 7.56 14.91	3.71 (4.83) 6.55 12.55	3.48 (4.47) 5.99 11.28	3.33 (4.24) 5.64 10.48
11	4.82 (6.72) 8.65 19.69	3.88 (5.26) 7.21 13.81	3.71 (4.83) 6.55 12.55	3.36 (4.28) 5.67 10.35	3.20 (4.04) 5.32 9.58
→12	4.75 (6.55) 9.33 18.64	3.89 (5.10) 6.93 12.97	3.49 (4.47) 5.95 10.80	**3.26** **(4.12)** **5.41** **9.63**	3.11 (3.89) 5.06 8.89

Table 9.14 shows the values of the F distribution for the treatments. In my project, the F Distribution value for the treatments is 2.33 (shown in Table 9.13), which is smaller than 3.26 (5%) found on Table 9.14. with

$v_1 = (n-1) = 4$, and $v_2 = (n-1)\ (n-2) = 12$ (Murdoch and Barnes, 1975).

This means that some of the fracture toughness values have an error of more than 5 percent. Therefore, not all treatments are acceptable. Test results of treatment for sample U (540 Watts and 15 seconds) seem to be the most acceptable as its fracture toughness mean is 48.32, which is closest to that of ambient cured (51.65). Comparing it with the previous experiment result of 180 W and 80 seconds (fracture toughness = 51.41), which is closer to the ambient cured (51.65). Therefore 180-W power and 80-second is more acceptable.

Other fracture toughness values of the composites cured under different conditions are summarized in Table 9.15, which shows that the value of the fracture toughness of the:
540 W and 15s microwave cured sample is lower than the ambient cured one by 6.9%.
540 W and 20 s microwave cured one is lower than the ambient cured one by 36.7%.
540 W and 25s microwave cured one is lower than the ambient cured one by 10.53%.
720 W and 15s microwave cured one is lower than the ambient cured one by 18.6%.
720 W and 20s microwave cured one is lower than the ambient cured one by 25.7%.
720 W and 25s microwave cured one is lower than the ambient cured one by 12.33%.

Table 9.17: Results of the fracture toughness and other parameters for VE cured under different conditions.

Condition	Ambient	180 Watt		360 Watt		540 Watt			720 Watt		
Time	Nil	60s	80s	60s	80s	15s	20s	25s	15s	20s	25s
Elongation at Peak (mm)	1.214	1.254	1.162	1.234	1.121	1.07	0.93	1.23	1.232	1.043	1.167
Peak Load (N)	1365.33	1389.67	1358.67	1264.17	1281.67	1273.6	995.8	1235	1148	1083	1212
Elongation at Break (mm)	1.520	1.557	1.518	1.478	1.445	1.32	1.25	1.592	1.806	1.206	1.556
Break Load (N)	1090.33	1119.17	897.33	1054.83	907.33	1034.2	701.4	833	788	900	885
Fracture toughness ($N.mm^{-3/2}$)	51.65	52.72	51.41	49.30	48.49	**48.32**	**37.78**	**46.73**	**43.54**	**41.08**	**45.98**

From the Table 9.17, it is obvious that the fracture toughness for the categories of 540-watt microwave power with 15 seconds, 20 seconds, 25 seconds of exposure times and 720-watt microwave power with 15 seconds, 20 seconds, and 25 seconds are much lower from the previous experimental results. The differences can be explained from many aspects such as the increasing of flaw. The result obtained is further investigated and proven by analyzing the micrographs of specimen using SEM.

9.5 SEM Analysis of Fractured Surface

The fractured surfaces of the samples were analyzed using a Scanning Electron Microscope (SEM). It was found that some area of the chevron edge cut showed the

ductile behaviour and some displayed the brittle behaviour. There were four critical points of the chevron fractured surface to be analyzed as illustrated in Figure 9.6.

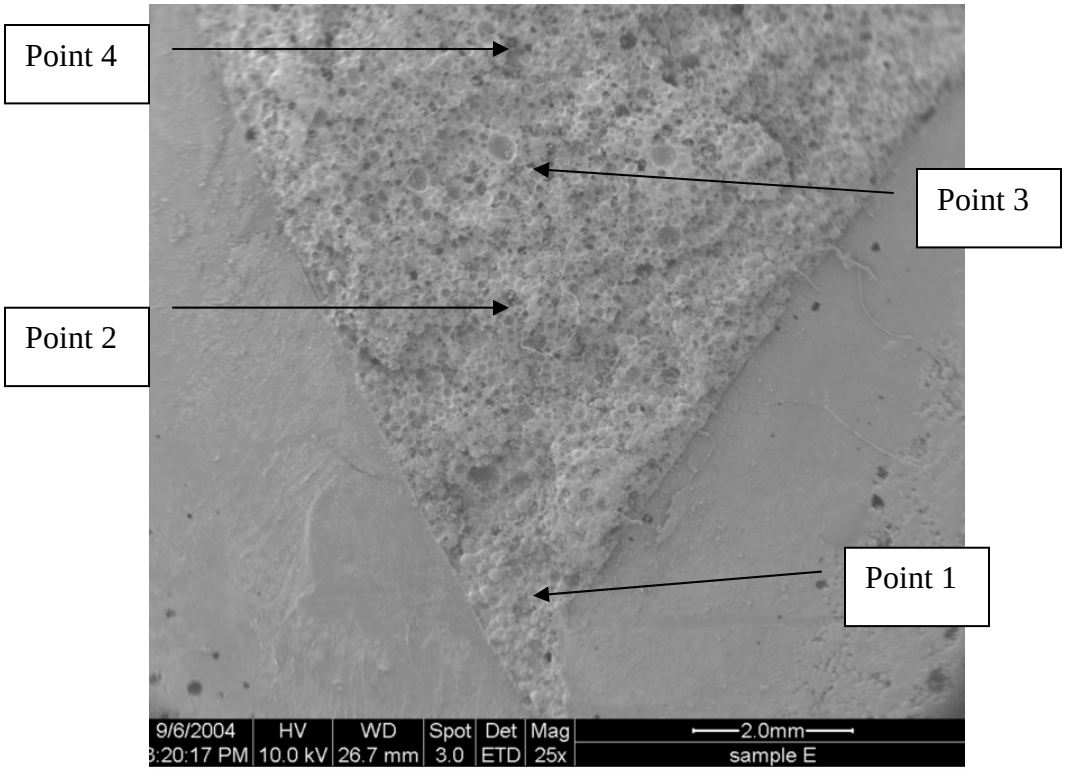

Figure 9.6: Micrograph showing the sample with chevron cut by magnification 25x

Two specimens were chosen for investigation because it took a long time to use the scanning electron microscopy for analyzing a specimen. The specimen chosen were from the categories of 540-watt microwave power with 25 seconds (higher fracture toughness value) and 720-watt microwave power with 20 seconds. We expect that the fracture surface with higher value of K_{IC} would have lesser flaws than the specimen with lower value K_{IC}. It was anticipated that by using microwave heat-treatment on the samples, there might be some changes of the microstructure of samples. The changes would affect

the material properties like its fracture toughness. All other specimens micrograph as shown in Appendix D.

9.5.1 Higher Fracture Toughness Value Specimen

The specimen chosen was the 540 watts and 25 seconds because it possessed the higher value of fracture toughness. There are four critical points were analyzed by magnification up to 500 times as illustrated in Figures 9.7 through 9.10.

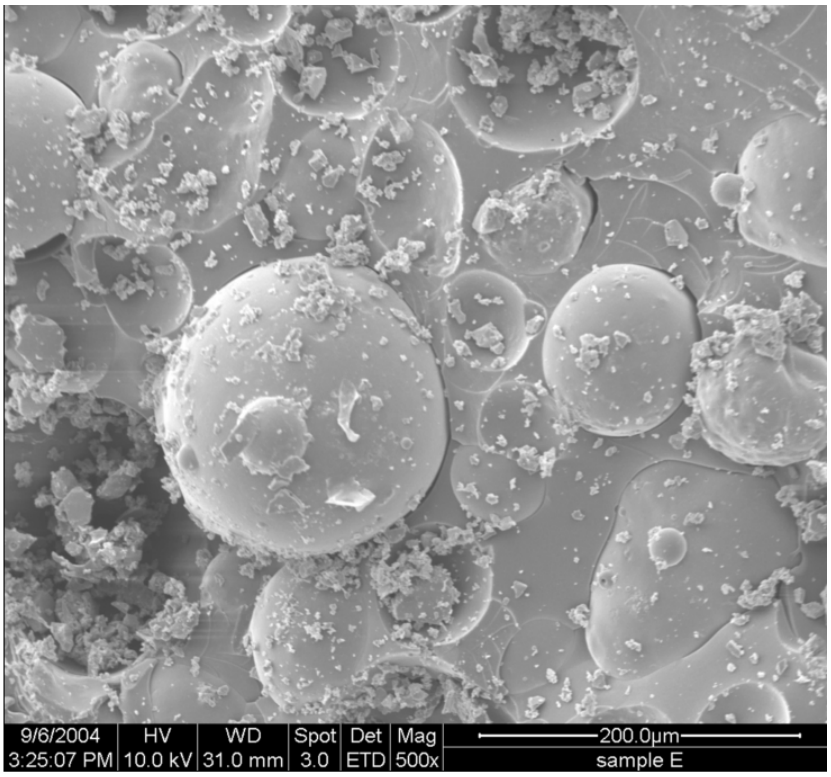

Figure 9.7: Micrograph of area 1 showing chevron cut by a magnification of 500 x.

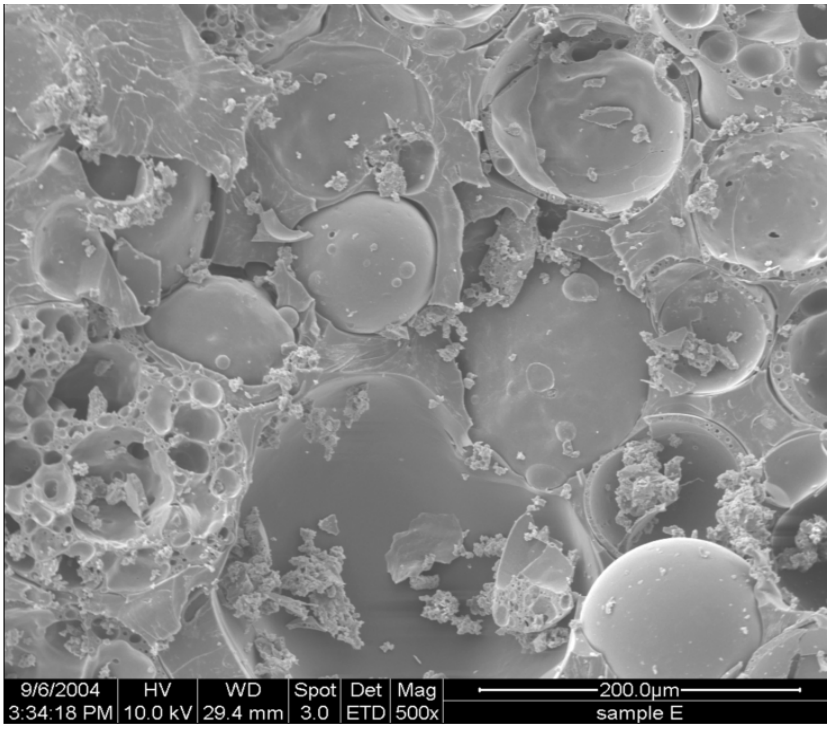

Figure 9.8: Micrograph of area 2, the stretch-zone by a magnification of 500 x.

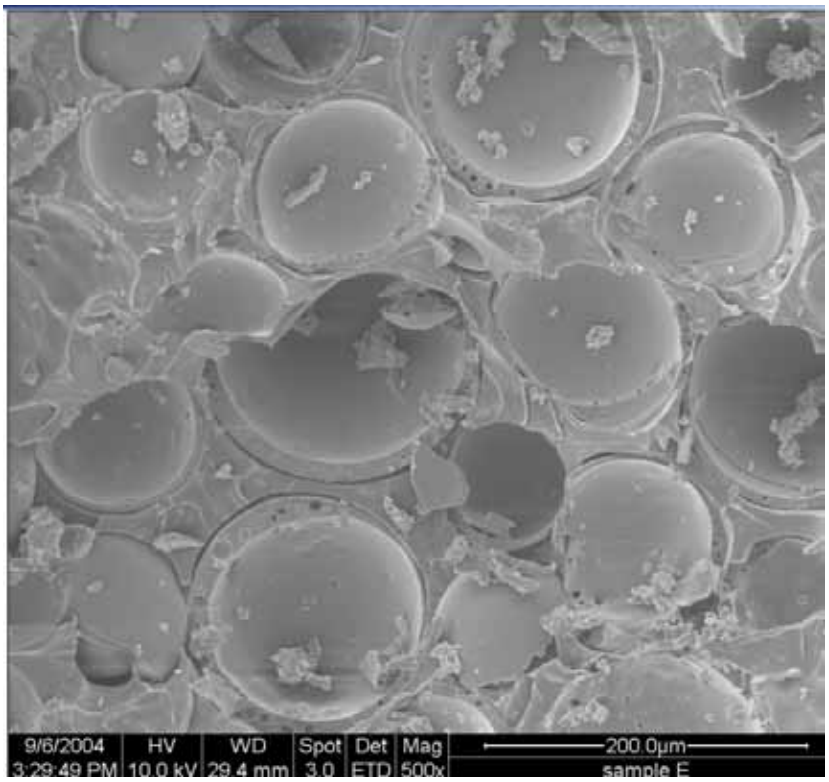

Figure 9.9: Micrograph of area 3 showing some scratches on the fractured surface by a magnification of 500 x.

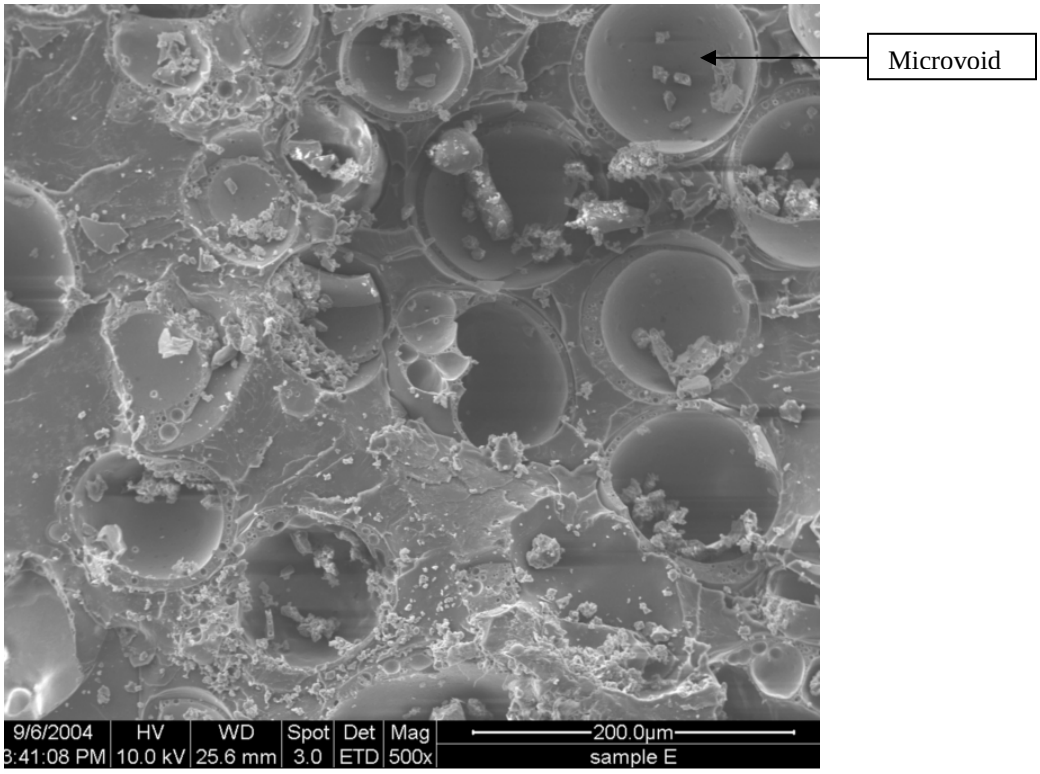

Figure 9.10: Micrograph of area 4 showing some microvoid on the fractured surface by a magnification of 500 x.

9.5.2 Lower Fracture Toughness Value Specimen

The specimen chosen was the 720-watt power level and 20 second-exposure time because it possesses the lower value of fractured toughness. There are four critical points of the fractured surface to be analyzed as shown in Figure 9.11 Those critical points were analyzed by a magnification up to 500 times as illustrated in Figures 12 through 17.

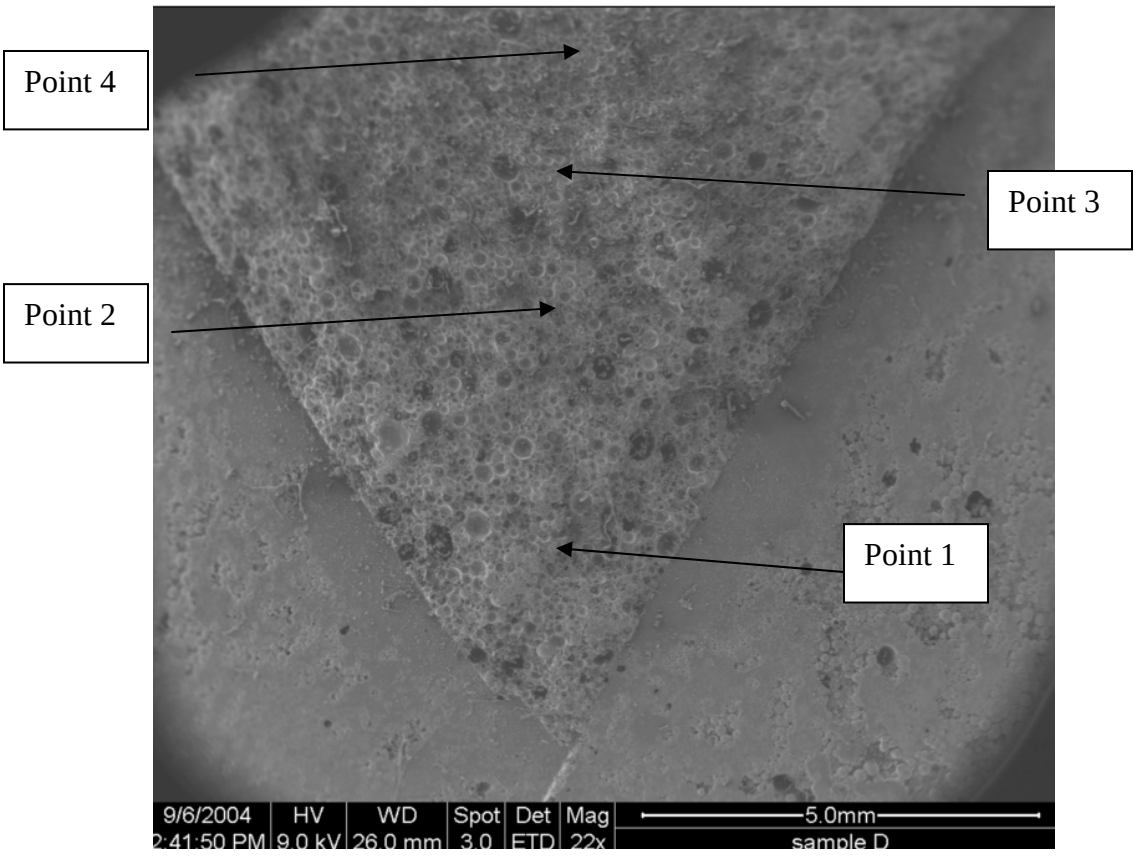

Figure 9.11: Micrograph showing the sample with chevron cut by a magnification of 25x

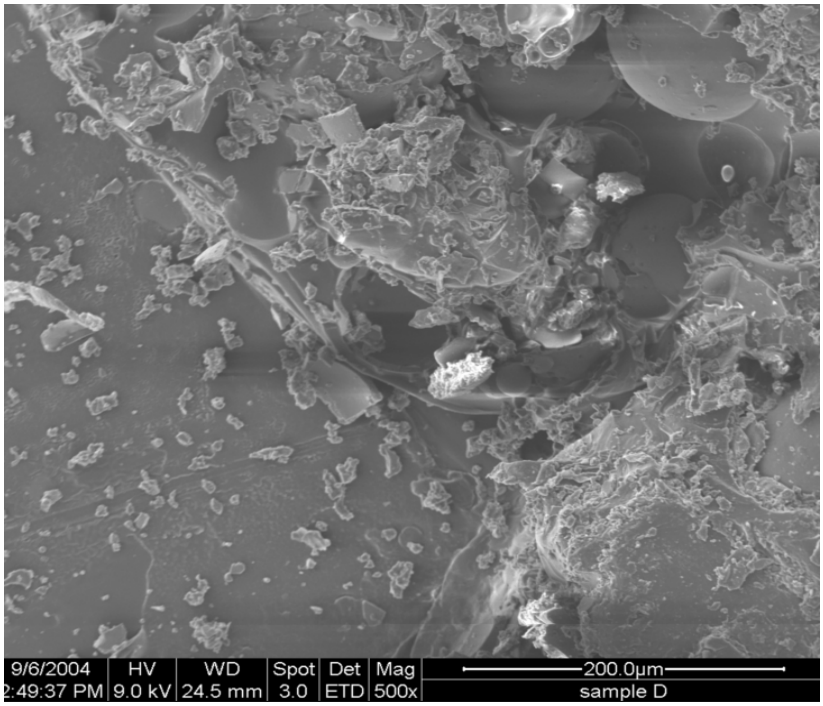

Figure 9.12: Micrograph of point 1 showing the eight crack points by a magnification of 500 x

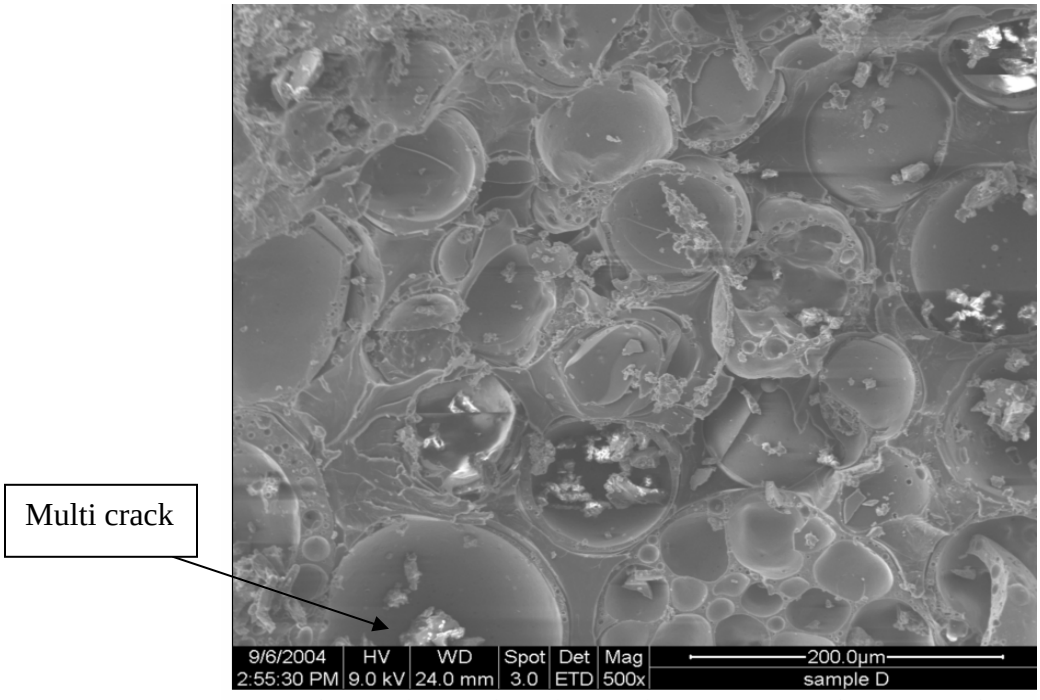

Figure 9.13: Micrograph of point 2 showing the multi crack by a magnification of 500 x

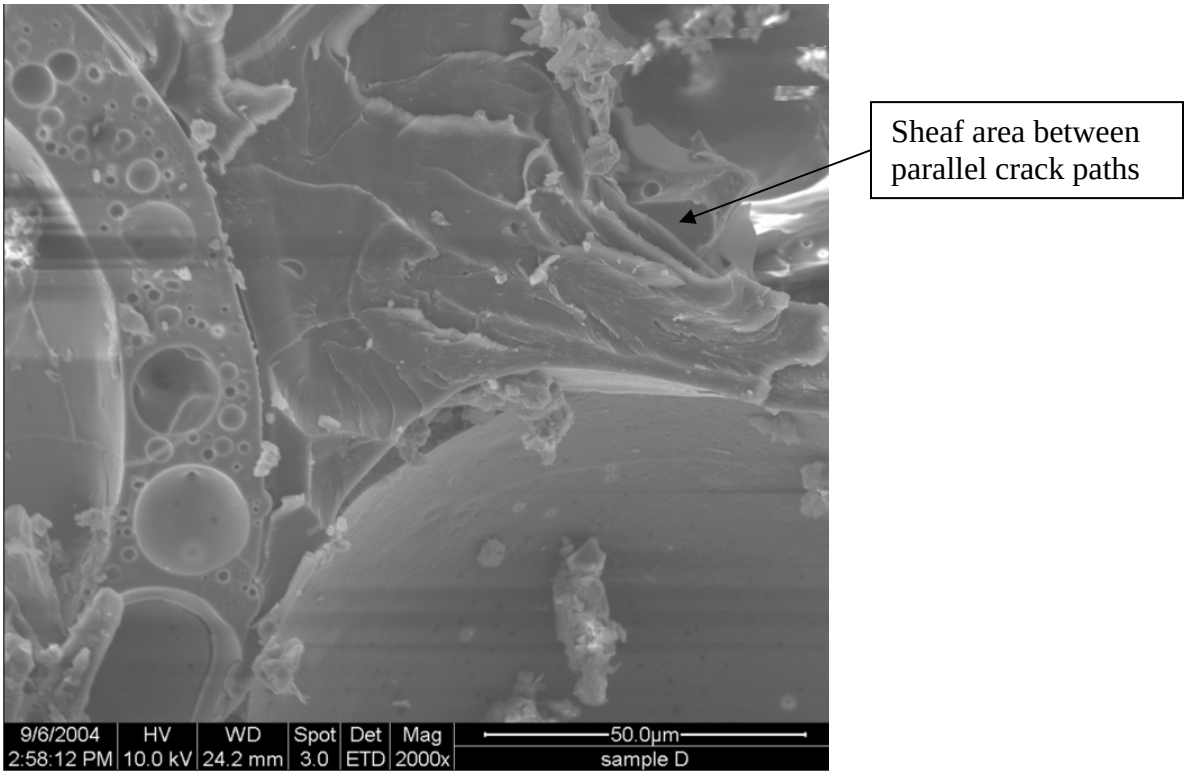

Figure 9.14: Micrograph of point 2 zoomed in the multi crack area by a magnification of 200 0x

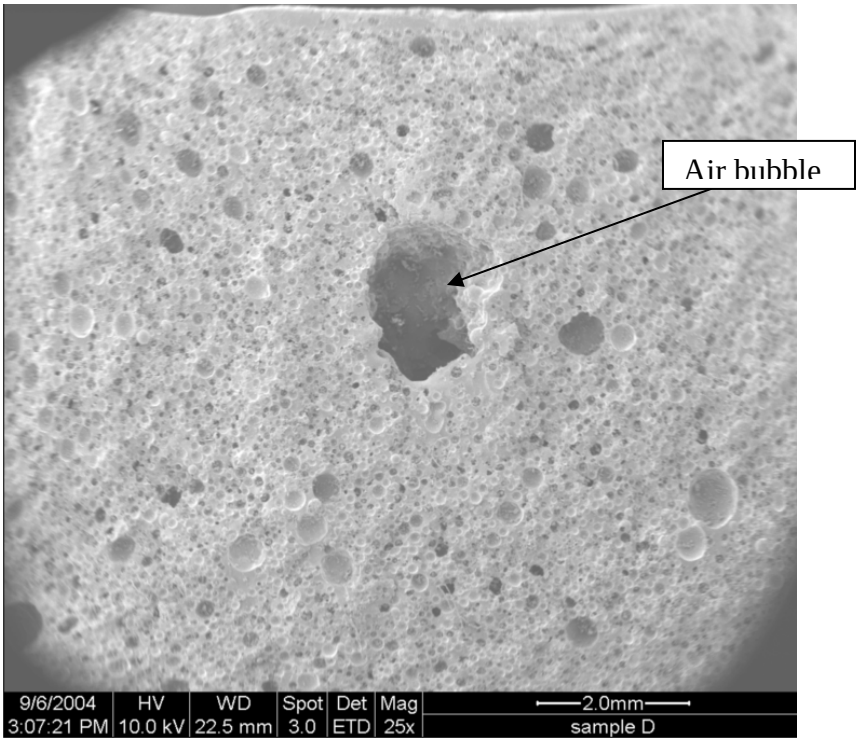

Figure 9.15: Micrograph of point 3 showing the air bubble by a magnification of 25 x

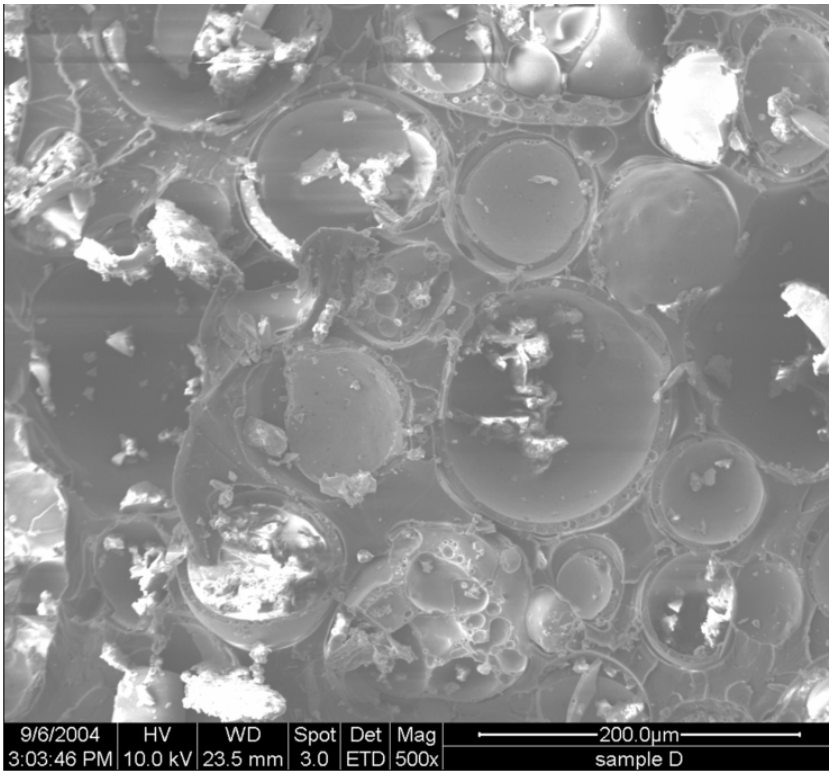

Figure 9.16: Micrograph of point 3 zoomed in the air bubble area by a magnification of 500 x

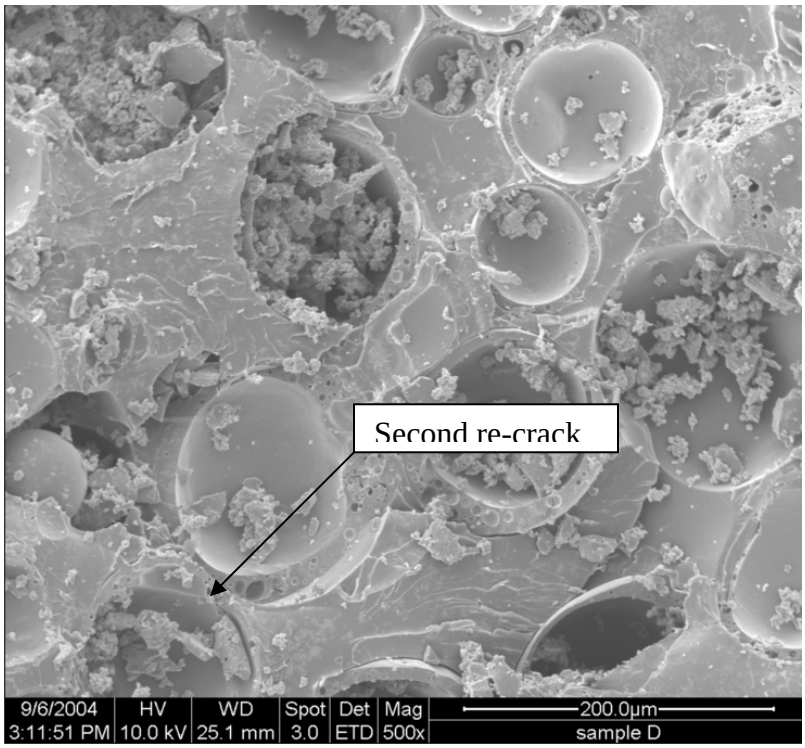

Figure 9.17: Micrograph of point 4 showing the second re-crack by a magnification of 500 x

Chapter 10. Conclusion and Recommendations

10.1 Conclusion

The short bar test can be used effectively in the prediction of fracture toughness value of vinyl ester composite. This can only be done if it meets the requirement of specimen that well constructed; otherwise, the crack jump may occur. This is because of its manufacturing defect or mistakes in preparing the short bar specimen. The new method of preparing the short bar specimen with a non-metallic mould is found to be acceptable and executable. Even if there are variations in each specimen, the variations however are still within the tolerance limits. The disadvantages of the mould fabricating are time-consuming and it is not recyclable. As a consequence the design and material have to be improved so that the mould can be recycled in order to enhance its application to manufacturing industry in the future.

The fracture toughness values for the samples cured under 180W and 80-second exposure are the closest to the mean value of ambient condition. The treatment of 180W and 80 second exposure time are the most acceptable and suitable treatment to used in order to reduce the shrinkage of vinyl ester composite.

The fracture toughness of vinyl ester composites varies slightly after undergoing the microwave treatment. It varies with different microwave power level and duration of exposure. It is also concluded that the 180-watt and 60-second combination produced the

highest value of fracture toughness and it seems to be very stable even if the exposure time is increased to 80 seconds. However, it is noticeable that the value of fracture toughness changes rapidly as the power level increased to 360 Watts. The change is significant and the treatment with more than 180-Watt power level is not recommended. Further explanation on the fracture surface analysis is based on the use of scanning electron microscopy. Even though the results obtained from the SEM analysis is not very obvious; they still show some of the important features such as: brittle behaviour, elongation of the fracture surface of vinyl ester composite. The sample with lower fracture toughness is found to have more bubbles in the composite than those samples with higher fracture toughness. Therefore, the microwave power level and exposure time appear to correlate with the K_{ICSB} values obtained

10.2 Recommendations

The results can be improved throughout the following efforts:

- Improve material properties of the mould and structure of specimen: By using a better material especially the slot part should be made of harder material so that the part would not be bent aside. Meanwhile the teeth on the edges of specimen must be clean; moreover the load line surface must be flat in order to provide an accurate and consistent results.

- Maintenance of specimen after tensile testing: A few of the micrographs acquired shows that the surface of chevron cut deteriorated by scratching or compressing it with the other materials. These actions might damage the important features of the crack as shown on the chevron surface, thus the specimens are suggested to keep in a solid container and they should be taken for SEM (Scanning Electron Microscope) testing as soon as possible after the tensile testing.

- Simulation: More information can be obtained if computer software is used to analyse the experimental results, such as: the area of maximum fracture toughness and etc. The software package called ANSYS is suggested because it is user-friendly and it can be incorporated with other software such as PRO-ENGINEER and so on.

List of References

Askeland, D R, 1998, *The Science and Engineering of Materials*, 3rd edn, Stanley Thornes.

Astrom, B T 1997, *Manufacturing of Polymer Composites*, Chapman and Hall, United Kingdom

Baddeley, D T and Ballard J, 1991, *Evaluate the Short Rod/Bar Fracture Mechanics Test*, BEng Thesis of Jennine Ballard, School of Mechanical and Manufacturing Engineering, Queensland University of Technology, Australia.

Barker, L M, 1979, *Fracture Mechanics Applied to Brittle Materials*, ASTM, STP 678, American Society for Testing and Materials.

Baker, L M, 1980, *Development of the Short Road Method of Fracture Toughness Measurement, Proceedings, Conference on Wear and Fracture Prevention,* 21-22 May 1980, ASM, Metals Park, Ohio, pp. 163-180.

Baker, L M, 1981, *Short Rod and Short Bar Fracture Toughness Specimen Geometries and Test Methods for Metallic Materials, Proceedings, Fracture Mechanics:* Thirteenth Conference, ASMT STP 743, 1981, pp. 456-475.

Bolton, W, 1996, *Materials and Their Uses*, Butterworth and Heinemann, p. 128.

Callister, W D, 2003, *Materials Science and Engineering*: *An Introduction*, 6th edn, John Wiley and Sons, Inc., pp. 201-203.

Clarke, J L Editor, 1996, Structural design of polymer composites, E & FN Spon, United Kingdom.

Denes, J and Keedwell, A D, 1974, *Latin Squares and their Applications*, English University Press Ltd., pp.1-41.

DiJon Inc., Technical Note 503: *The Advantage of the Short Rod Test Method*. (n.d.), viewed 8 June 2004 <http://www.dijoninc.com/home.html>.

Fibre Glast Development Corporation, *MSDS Promoted vinylester resin (n.d.), viewed 27 June 2004* <www.fibreglast.com/msds/01110.html>.

J. Thuery, 1992, *Microwaves Industrial, Scientific and Medical Applications*, Artech House, Inc., United Kingdom.

James H. Hanson, 1997, *The Short Rod: The Potential Test Method For Determining The Fracture Toughness of Concrete*, viewed 1 July 2004, <http://www.cfg.cornell.edu/reference/presentations/SHPE/SHPE6.html>.

Ku, H S, Siores, E, Ball, J A R and Horsfield, B (1999a), Microwave Processing and Permittivity Measurement of Thermoplastic Composites at Elevated Temperatures, Journal of Materials Processing Technology, United States of America, Vol. 89-90, pp. 419-24.

Ku, H S, Siores, E, Ball, J A R (1999b), Microwave Facilities for Welding Thermoplastic Composites, and Preliminary Results, Journal of Microwave Power and Electromagnetic Energy, United States of America, Vol. 34, No. 4, pp. 195-205.

Ku, H S, Siores, E, Ball, J A R and Horsfiled, B (2001), Permittivity Measurement of Thermoplastic Composites at Elevated Temperature, Journal of Microwave Power and Electromagnetic Energy, United States of America, Vol. 36, No. 2, pp. 101-111.

Ku, H S, Van Erp, G, Ball, J A R and Ayers, S (2002a), Shrinkage Reduction of Thermoset Fibre Composites during Hardening using Microwaves Irradiation for Curing, Proceedings, Second World Engineering Congress, Kuching, Malaysia, 22-25 July, pp. 177-182.

Ku, H S (2002b), Risks involved in curing vinyl ester resins using microwaves irradiation, Journal of Material Synthesis and Processing, Vol. 10, No. 2, pp. 97 - 106.

Matthews, F L and Rawlings, R.D, 1994, *Composite Materials: Engineering and Science*, 1st edn, Chapman and Hall, United Kingdom.

Metaxas, A C. and Meredith, R J, 1983, *Industrial Microwave Heating*, Peter Peregrinus Ltd., pp. 5-6, 28-31, 43, 211, 217, 278, 284-5.

Museum of Science, 1996, *Scanning Electron Microscope*, viewed 24 July 2004, <http://www.mos.org/sln/sem/intro.html>.

Munz, D, 1981, *Determination of Fracture Toughness of High Strength Aluminum Alloys with Cheron Notched Short Rod and Short Bar Specimens*, Engineering Fracture Mechanics, Vol. 15, No. 1-2, pp. 231-236.

Murdoch, J and Barnes, J A, 1975, *Statistical Tables for Science, Engineering and Management*, Macmillan, p.9.

National Research Council (NRC), 1994, *Microwave Processing of Materials, National Materials Advisory Board, Commission on Engineering and Technical Systems*, National Academy Press, United States of America.

Osswald, T A and Menges, G, 1995, *Materials Science of Polymers for Engineers*, Hanser Publishers, New York.

Peters, S T, 1998, *Handbook of Composites*, Chapman and Hall, United Kingdom.

Pritchard, G, 1999, *Reinforced Pastics Drability*, Woodhead publishing Ltd., United Kingdom.

SIRC (Styrene Research and Information Centre), 1998, *Information on the Regulatory Treatment of Styrene*, viewed 20 September 2004, <http://www.styrene.org/sircreg2.html>.

TerraTeck Inc, *Short Rod Fracture Toughness Test System* (n.d.), viewed 2 August 2004, <www.terratek.com/equipment/fracto_2.htm>.

Sweet, J R Co., *MSDS for MEKP*, (n.d.), viewed 22 August 2004, <www.johnrsweet.com/mekp/html>.

University of Denver, *Latin Squares* (n.d.), viewed 28 July, <www.du.edu/~jcalvert/econ/latsqar.htm>.